FOMC Announcements and Global Interest Rate Expectations

Zehao Li*

December 2023

Abstract

Secular declines in global sovereign yields are concentrated in short event windows around U.S. monetary policy announcement dates. Cumulative changes in sovereign yields during FOMC announcement dates contain critical information for explaining the persistent variations in the yields, predicting future yields and excess bond returns, and determining interest rate expectations and term premia. We build a dynamic term structure model with shifting endpoints to study the effects of U.S. monetary policy on world yield curves. Our findings highlight that U.S. monetary policy drives the secular declines in global interest rates by reducing expected interest rates.

Keywords: U.S. monetary policy, yield curve, global financial cycle.
JEL Codes: E43, E52, F42

*The Chinese University of Hong Kong, Shenzhen. Address: 2001 Longxiang Blvd, Longgang District, Shenzhen, Guangdong, China. Email: lizehao@cuhk.edu.cn.

1 Introduction

Nominal sovereign yields in advanced economies have exhibited a steady decline since 1990. Traditional explanations attribute these declines to slow-moving macroeconomic trends, such as demographic shifts, slowing economic growth, and a global savings glut. Accordingly, long-term declines in interest rates should not discriminate certain sets of dates against others in a year. However, this paper reveals that secular declines in global interest rates are concentrated within specific event windows while remaining relatively stable on other dates. In particular, three-day event windows surrounding U.S. FOMC announcement dates, spanning from the day before to the day after, account for a significant portion of the observed secular declines in world sovereign yields.

This paper revolves around the empirical patterns depicted in Figure 1, which illustrates the dynamics of 10-year nominal sovereign yields during three-day event windows surrounding U.S. Federal Open Market Committee (FOMC) announcement dates for G10 countries and Denmark. Fluctuations in world interest rates are highly concentrated in these event windows. We adjust the initial values of the time series to start at zero so the time series can be interpreted as cumulative changes since the initial period. Furthermore, we sum the daily changes in the 10-year yields within or outside the three-day windows around U.S. FOMC announcement dates. For the U.S., the cumulative sum of daily changes within FOMC windows closely aligns with the original 10-year yield series, while the cumulative changes outside the FOMC windows remain stable around zero. This replicates Figure 1 of Hillenbrand (2021). Remarkably, we observe similar patterns for other countries. The cumulative changes in sovereign yields during U.S. FOMC announcement windows fit the original sovereign yield series very well, while dates outside the FOMC announcement windows appear less relevant for the secular variations in sovereign yields. Despite U.S. monetary policy primarily targeting domestic interest rates and FOMC announcement windows representing less than 10% of total business days per year, these short event windows are critical for determining the long-term behaviors of world interest rates.

In this paper, we study how the *cumulative* effects of U.S. monetary policy shape global yield curves by exploiting the cointegration patterns in Figure 1. We emphasize that U.S. monetary policy announcements play a significant role in forming interest rate expectations worldwide. Furthermore, we stress that the long-term declines observed in global interest

Figure 1: FOMC announcement dates and 10-year sovereign yields.

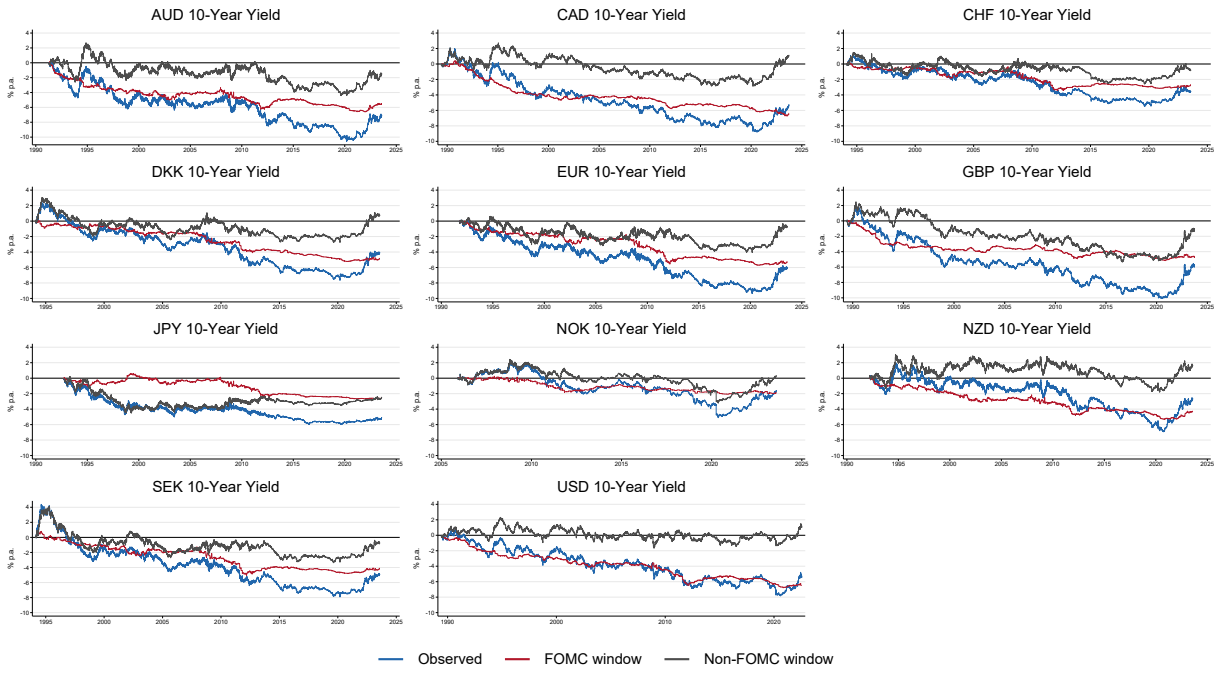

Notes: The figure shows that 3-day event windows around FOMC announcements capture substantial proportions of variations in observed global interest rates. Each FOMC window ranges from the day before to the day after an FOMC announcement date. Non-FOMC windows are the days outside the FOMC windows. Observed: observed 10-year nominal sovereign yield. FOMC window: cumulative changes in the 10-year yield incorporating only daily changes during the FOMC windows. Non-FOMC window: cumulative changes in the 10-year yield without daily changes during the FOMC windows.

rates are primarily due to reductions in expected interest rates rather than term premia. We proceed in two steps. First, we establish some empirical facts regarding the relationship between the cumulative effects of U.S. monetary policy announcements and world interest rates. Second, to account for these facts, we build and estimate a dynamic term structure model that embeds an I(1) trend in the state variables. Relating the trend to the cumulative effects of U.S. monetary policy, the model can replicate the key empirical facts. Importantly, the model offers new estimates of interest rate expectations and term premia worldwide and provides a new explanation of the secular declines in global interest rates.

We establish two new stylized facts about U.S. monetary policy announcements and world interest rates. First, we quantitatively establish the cointegration relationship between world interest rates and their cumulative responses to U.S. monetary policy announcements presented in Figure 1. It is well-known that interest rates are highly persistent, and interest rates of different maturities contain a common trend component. We show that this trend can be well approximated by the cumulative changes in yields during the FOMC announcement windows averaged across all maturities. Since the changes in worldwide interest rates are synchronized during the U.S. monetary policy announcement windows, the cumulative changes in the U.S. yields and domestic yields during the FOMC windows provide similar approximations for the cointegration trend of each country's yield curve. The cointegration relationship implies that the cumulative effects of the U.S. monetary policy announcements are an important reference for predicting future interest rates. Whenever the sovereign yields deviate from this trend, they are expected to revert.

The second stylized fact is that the cumulative effects of U.S. monetary policy announcements are crucial for understanding bond risk premia. Relative to the canonical predictive regressions for excess bond returns only using current yields as predictors, our baseline regressions substantially improve the predictive power by incorporating the cumulative yield changes during FOMC announcement windows as additional predictors. This improvement arises from the ability of the cointegration errors in sovereign yields to significantly predict excess bond returns. Furthermore, the cumulative changes in sovereign yields outside the FOMC windows are good proxies for the cointegration errors relative to the cumulative yield changes during FOMC windows, and using these changes as predictors achieves similar predictive power as the baseline regressions. These facts imply that the cumulative yield changes during FOMC announcement windows capture the expectations hypothesis

component of worldwide sovereign yields.

Furthermore, we orthogonalize the cumulative effects of FOMC announcements by sovereign yields and use the residuals to predict excess bond returns. The predictive power is comparable to or even higher than that of the currently observed yields. Therefore, the cumulative effects of FOMC announcements also contain rich information about the bond risk premia orthogonal to current yields. Jotikasthira et al. (2015) argue that bond yields in major economies are highly synchronized because of positively correlated term premia. They also find that the level of U.S. yields contributes substantially to the risk compensation channel of global yield comovements. Consistently, our regressions also suggest that U.S. interest rates are related to global bond risk premia. However, we emphasize that global bond risk premia are related to the cumulative changes in U.S. interest rates within short event windows around FOMC announcements instead of the raw level of observed yields.

To account for these stylized facts, we build a dynamic term structure model with a shifting endpoint for interest rates. The endpoint refers to the long-term limit of interest rate expectations, which is constant in canonical stationary affine term structure models (e.g., Joslin et al. (2011), Joslin et al. (2014), Adrian et al. (2013), and Wright (2011)). It is important to allow for shifting endpoints because our empirical analysis implies that the series capturing the expectations hypothesis component also approximates the cointegration trend of interest rates, which trends downward. Consistent with the empirical facts, our model implies that the secular declines in interest rates are mainly due to reductions in interest rate expectations. Fixed endpoint models attribute the persistent declines in interest rates to falling risk premia because long-term expectations of interest rates must converge to the unconditional mean.

The shifting endpoint model follows Bauer and Rudebusch (2020), but we use the sovereign yields' cumulative responses to U.S. monetary policy announcements as empirical proxies for the endpoint. We also consider multiple proxy variables for the endpoint to jointly study the roles of cumulative changes in domestic and U.S. interest rates during the FOMC windows for world yield curves.

The shifting endpoints model naturally implies a cointegration trend for the yield curve. We demonstrate that cumulative yield changes during FOMC windows effectively capture the model-implied interest rate trends (referred to as OSE in Bauer and Rudebusch (2020)), successfully replicating the key empirical facts. As a robustness check, we also compare the

trends inferred from observed yields (referred to as ESE in Bauer and Rudebusch (2020)) with the trends estimated using the OSE method. We find remarkable similarities between the trends estimated using both methods, strengthening our analysis.

We employ the shifting endpoint model to conduct two exercises. First, we investigate the driving forces of secular declines in interest rates worldwide in the spirit of Wright (2011). Second, we estimate the cumulative effects of U.S. monetary policy announcements on world risk-neutral rates and term premia.

In the first exercise, our shifting endpoint model attributes the downward trend in global interest rates primarily to decreasing interest rate expectations, driven by cumulative sovereign yield changes during FOMC announcement windows. Furthermore, it indicates more pronounced cyclical variations in term premia compared to Wright (2011) and Bauer et al. (2014). Notably, our model captures significant surges in term premia during the Global Financial Crisis, a feature that fixed endpoint models cannot replicate.

Our OSE model accommodates vector-valued shifting endpoints by incorporating cumulative changes in both domestic and U.S. interest rates during FOMC windows as proxies. For Canada, Switzerland, the U.K., and Norway, the interest rate trends are primarily influenced by the cumulative changes in *U.S.* interest rates during the FOMC windows, aligning with the standard global financial cycle argument of *U.S.* monetary policy shocks affecting other countries' interest rates. For Australia, Denmark, Germany, New Zealand, and Sweden, the interest rate trends are predominantly driven by the cumulative changes in *domestic* interest rates during the FOMC windows. While not directly shaped by U.S. monetary policy shocks per se, these trends still reflect dynamics associated with U.S. monetary policy announcements. As U.S. monetary policy announcement dates rarely coincide with those of other countries (Albagli et al. (2019)), changes in domestic interest rates during FOMC announcement windows can be interpreted as effects of U.S. monetary policy announcements. Our results generalize the findings of the global financial cycle literature, offering a broader perspective by incorporating both U.S. and domestic interest rate responses to monetary policy announcements as independent variables rather than relying solely on changes in U.S. interest rates during FOMC windows.

In our second exercise, we employ the shifting endpoint model to estimate risk-neutral rates and term premia. We then calculate the cumulative changes in these rates during FOMC windows or other dates. Our analysis reveals that risk-neutral rate fluctuations

are predominantly concentrated within FOMC windows across all countries in our sample. Interestingly, this phenomenon is more pronounced for some non-U.S. countries than for the United States itself. Furthermore, the impacts of FOMC announcements on risk-neutral rates increase with maturity. In contrast, term premia exhibit much greater variations outside FOMC windows. Therefore, U.S. monetary policy is vital in determining global risk-neutral rates, while other /factors influence term premia.

Expected interest rates are key to monetary policy transmission in standard new Keynesian theories. Shifting endpoints are essential for generating large cumulative responses of world risk-neutral rates to U.S. monetary policy announcements. Our shifting endpoints model implies that the cumulative changes in world risk-neutral rates during FOMC windows are at least twice as large as estimates from traditional fixed endpoint term structure models (e.g., Adrian et al. (2013)).

Related Literature This paper contributes to the global financial cycle literature. The literature identifies U.S. monetary policy as a critical driver of global financial cycles, for example, Albagli et al. (2019), Rey (2015), Miranda-Agrippino and Rey (2020), Miranda-Agrippino and Rey (2022), Albagli et al. (2019), Del Negro et al. (2019), Dedola et al. (2017), Jarociński (2022), and Gerko and Rey (2017). Non-U.S. central banks fail to fully offset the spillover effects of U.S. monetary policy shocks due to fluctuations in risk premia and financial conditions imported from the U.S.

Our study integrates the previously distinct realms of high-frequency monetary policy shock literature (e.g., Gürkaynak et al. (2005a), Gürkaynak et al. (2005b), Hanson and Stein (2015), Nakamura and Steinsson (2018), Bauer and Swanson (2022) and the aforementioned papers on global financial cycles) and research on secular interest rate trends (e.g., Laubach and Williams (2003), Holston et al. (2017), Del Negro et al. (2017b, 2019)). Regarding the spillover mechanism, Albagli et al. (2019) find the effects of U.S. monetary policy shocks on developed economy bond yields concentrated in risk-neutral rates. While empirical studies have traditionally examined the *marginal* effects of monetary policy shocks through approaches such as local projections or structural VARs, our results suggest that the *cumulative* total effects of these shocks explain remarkable proportions of the secular declines in global interest rates.

The secular declines in interest rates have drawn wide attention. Prominent explana-

tions of the secular declines include the global savings glut (Bernanke (2005), Bernanke et al. (2011)), safety and liquidity of Treasury securities (Caballero et al. (2008), Krishnamurthy and Vissing-Jorgensen (2012), Del Negro et al. (2017b, 2019), Greenwood and Vayanos (2014)), limited capital investment opportunities (Summers (2014)), lower economic growth (Gordon (2017), Del Negro et al. (2019)), declining capital prices (Eichengreen (2015)), and demographic changes (Gagnon et al. (2021), Carvalho et al. (2016)). These explanations do not discriminate any dates from others and thus imply the secular decline in interest rates should be evenly distributed over time. However, Hillenbrand (2021) demonstrates that only the FOMC announcement windows matter for the secular declines in U.S. Treasury yields since 1990. Building on his work, we show that short event windows around FOMC announcement dates are also disproportionately critical for the declines in global interest rates.

We also contribute to the estimation of bond risk premia in a global context. Previous research, such as Wright (2011), has attributed the secular declines in world interest rates to reductions in term premia. Jotikasthira et al. (2015) demonstrate the significant roles of world inflation and U.S. yield level in determining the covariance of global interest rates, primarily through the risk compensation channel. Recently, Bauer and Rudebusch (2020) argue that the stationary term structure models imply excessive dynamics in the risk premia because the interest rate expectations are too stable by construction. Allowing for a persistent trend in the state vector reverses the decomposition results. Consistent with Bauer and Rudebusch (2020), our shifting endpoint model implies that the interest rate expectation channel is much more important for the secular declines in world interest rates than the previous literature has found. Moreover, the persistent variations in nominal yields have been widely attributed to the dynamics of inflation (e.g., Wright (2011), Cieslak and Povala (2015), Jotikasthira et al. (2015)). We demonstrate that U.S. monetary policy better explains the persistent dynamics of world interest rates.

The rest of the paper is organized as follows. Section 2 describes the sovereign yields and FOMC announcement windows. Section 3 presents the stylized facts that are central to this paper. Section 4 presents the dynamic term structure model with shifting endpoints. Section 5 shows that U.S. monetary policy announcements are crucial for determining global interest rate trends and term premia according to the term structure model. Section 6 shows the cumulative effects of U.S. monetary policy announcements on global risk-neutral rates

Table 1: Sources of daily sovereign yields.

Country	Abbreviation	Source	Start
Australia	AUD	Bloomberg and author's calculations	Apr 16, 1991
Canada	CAD	Bank of Canada	Jan 2, 1986
Switzerland	CHF	Bloomberg and author's calculations	Feb 25, 1994
Denmark	DKK	Bloomberg and author's calculations	Feb 25, 1994
Germany	EUR	Bloomberg and author's calculations	Oct 03, 1991
U.K.	GBP	Bloomberg and author's calculations	Apr 16, 1991
Japan	JPY	Bloomberg and author's calculations	Sep 30, 1992
Norway	NOK	Bloomberg and author's calculations	Mar 7, 2012
New Zealand	NZD	Bloomberg and author's calculations	Mar 9, 1992
Sweden	SEK	Bloomberg and author's calculations	Feb 25, 1994
U.S.	USD	Federal Reserve Board (GSW)	Jun 14, 1961

Notes: GSW refers to Gürkaynak et al. (2007).

and term premia. Section 7 concludes.

2 Data

2.1 Daily Sovereign Yields

Our main source of daily sovereign yields is Bloomberg, which is also adopted by Du et al. (2018). Central banks such as the Federal Reserve Board and the Bank of Canada provide daily sovereign yields on their websites with starting dates earlier than the Bloomberg data. In this case, we use the yield curve data provided by the central bank[1]. Table 1 summarizes the sources of daily sovereign yields and the respective starting dates. For each country, the Bloomberg yield curve dataset contains maturities of 3 months, 6 months, and yearly maturities from 1 to 10 years. Bank of Canada's daily yield curve data covers maturities from 3 months to 30 years with quarterly increments. Gürkaynak et al. (2007) covers maturities from 1 year to 30 years with yearly increments. We augment the Gürkaynak et al. (2007) yield curve data with 3-month and 6-month interest rate data from the FRED. For Canada and the U.S., we select the same maturities as Bloomberg to be consistent with other countries.

[1]The Bank of England also provides daily yield curve data dating back to 1979, but the short-maturity yields were missing for early observations. So we adopt Bloomberg data.

2.2 FOMC Announcement Dates

The Federal Open Market Committee (FOMC) makes U.S. monetary policy decisions. Since 1981, the FOMC has typically held eight scheduled meetings per year. Most monetary policy decisions since 1994 have been made during these *scheduled* meetings, while a few were made during *unscheduled* meetings. In contrast, unscheduled meetings accounted for a large fraction of changes in the federal funds rate before 1994. Some of the unscheduled meetings were not followed by immediate policy actions or a statement. The public learned about these meetings with a significant time lag. These meetings are excluded from the list of FOMC announcement dates.

In line with Hillenbrand (2021), our selection of FOMC announcement dates corresponds to the time when the public receives information about the meetings. Before 1994, changes in monetary policy were typically disclosed to the market one day after the meeting through open market operations. Therefore, for dates before 1994, we rely on the dates that the market associated with a monetary policy change, as identified by Kuttner (2001, 2003). The main sample starts in June 1989. After 1994, monetary policy decisions were predominantly made during scheduled FOMC meetings, with the Fed consistently releasing a statement if the federal funds rate changed. Consequently, we utilize the dates when these statements were released. In Appendix A, we list the FOMC announcement dates.

3 FOMC and Global Interest Rate Trends: Stylized Facts

3.1 The FOMC Filter

Hanson and Stein (2015) uses changes from the day before to the day after FOMC meetings to capture the full market response to U.S. monetary policy shocks. In line with this approach, we interpret the changes in U.S. and world interest rates during these event windows as the responses to U.S. monetary policy shocks.

We apply the Hillenbrand (2021) filter to daily sovereign local currency yields. The filter divides the sample into two parts: FOMC windows consisting of dates $t-1, t, t+1$ for each FOMC announcement date t, and non-FOMC windows consisting of the other dates.

Then, the filter computes the cumulative sums of daily yield changes on each subsample. Equivalently, the filter assumes that the yields only change within a given subsample and remain constant on the other. Following Hillenbrand (2021), our FOMC dates start from June 5, 1989. However, most of our daily sovereign yields start after 1990, so our sample for each country starts when both series become available.

Formally, the filter is defined as

$$\nabla y_t^{(n),W} = y_{t_0}^{(n)} + \sum_{s=t_0+1}^{t} \left(y_s^{(n)} - y_{s-1}^{(n)} \right) \mathbf{1}_W(s), \tag{1}$$

where t and s denote daily dates, t_0 is the first date of the sample, $y_s^{(n)}$ is the log n-year Treasury zero coupon yield on date s, $\mathbf{1}_W()$ is an indicator function for the set W, and $W \in \{FOMC, nonFOMC\}$ is either the set of FOMC window dates or remaining dates outside of the FOMC windows. For brevity, we denote the FOMC-window changes in the n-year yield by $\nabla y_t^{(n)}$ and the first principal component of the FOMC-window changes in all yields by ∇y_t, unless we need to distinguish the FOMC-window from the non-FOMC-window series. Equation (1) defines a daily series. We can then aggregate it to the monthly or quarterly frequency by, for example, taking the end-of-period observations.

As shown in Figure 1, substantial fractions of variations in domestic-currency sovereign yields occur when the U.S. Federal Reserve announces its monetary policy decisions. In the Appendix, we repeat the decomposition exercise for the 3-month yields, 5-year yields, and 5-by-5-year forward rates of the same set of countries. The patterns are remarkably similar: the FOMC windows account for substantial proportions of variations in world interest rates of all maturities. Since the 10-year yield is the average of the 5-year yield and the 5-by-5-year forward rate

$$y_t^{(10)} = \frac{1}{2} y_t^{(5)} + \frac{1}{2} f_t^{(5,5)},$$

the decomposition patterns suggest that all segments of the yield curve evenly share the cumulative effects of FOMC announcements.

Quantitatively, we analyze the proportion of long-run declines in sovereign yields occurring within FOMC windows. We calculate the difference in annual average levels at the end and beginning of the sample and repeat this calculation for cumulative yield changes during FOMC windows. The fraction of the latter compared to the former is then computed.

Table 2 presents cumulative changes in world interest rates for the full sample and during FOMC windows, focusing on 3-month, 5-year, and 10-year maturities. For medium-to-long-term yields, more than 50% of the long-run declines occur within FOMC windows. Notably, despite representing less than 10% of trading days, FOMC windows have a significant impact on global interest rate changes. While smaller proportions of total declines in 3-month yields occur during FOMC windows, these fractions remain disproportionately larger compared to the fraction of FOMC windows in total trading days. U.S. monetary policy announcements have a relatively smaller impact on global short-term interest rates compared to long-term rates, as central banks have more control over sovereign short-term rates, leading to less synchronization with U.S. policy rates.

Cumulative changes in yields during the FOMC windows inherit the factor structure of original yields. It is well-known that the first principal component of the yield curve summarizes the majority of the variation in yields and puts roughly equal weights on each yield, rendering the name "level factor". The first principal component of cumulative changes in yields during the FOMC windows, ∇y_t, has similar properties. Table 3 reports the weights ∇y_t puts on each $\nabla y_t^{(n)}$ and the percentage of variations explained by ∇y_t. For all countries, ∇y_t puts roughly equal weights on yields beyond the one-year maturity, and the weights on the short maturities are also similar to those on longer maturities for most countries. Moreover, ∇y_t explains more than 82% of the total variations in $\nabla y_t^{(n)}$ for all countries and more than 95% for Canada, Denmark, Germany (EUR), and the U.S. Therefore, ∇y_t can be interpreted as average cumulative changes in yields during the FOMC windows, and is a good summary of the cumulative responses of the sovereign yield curve to U.S. monetary policy announcements.

3.2 Cointegration Tests

It is well-known that nominal Treasury yields are persistent and can be modeled as unit-root processes. We investigate whether the sovereign yield trends are concentrated on U.S. monetary policy announcement dates using cointegration regressions and error correction models. Formally, we estimate a dynamic OLS regression for the cointegrated process $(y_t^{(n)}, \boldsymbol{\tau}_t)$:

$$y_t^{(n)} = \beta_0 + \boldsymbol{\gamma}^\top \boldsymbol{\tau}_t + u_t, \tag{2}$$

Table 2: Cumulative changes in sovereign yields.

	3-mo			5-yr			10-yr		
	Obs.	FOMC	%	Obs.	FOMC	%	Obs.	FOMC	%
AUD	-10.32	-2.48	24.04	-8.84	-5.73	64.80	-8.74	-6.36	72.75
CAD	-9.42	-5.46	58.00	-6.53	-7.70	118.07	-6.44	-6.19	96.03
CHF	-4.79	-3.28	68.48	-4.23	-2.66	62.86	-4.16	-2.97	71.49
DKK	-5.53	-3.24	58.61	-5.92	-4.77	80.51	-6.18	-4.99	80.80
EUR	-9.36	-4.07	43.44	-8.70	-5.36	61.68	-8.15	-5.51	67.65
GBP	-9.96	-3.88	38.92	-8.94	-3.33	37.18	-8.52	-3.43	40.25
JPY	-4.32	-1.50	34.64	-4.45	-2.01	45.14	-5.47	-2.63	48.07
NOK	-1.20	-3.37	281.45	-1.57	-2.31	147.09	-3.29	-1.77	53.94
NZD	-2.49	-1.49	59.67	-4.04	-3.17	78.48	-4.44	-5.09	114.50
SEK	-6.64	-2.95	44.44	-6.06	-4.35	71.86	-6.56	-4.50	68.60
USD	-7.64	-12.81	167.55	-6.36	-6.93	109.06	-6.22	-6.44	103.53
					Pre-2008				
AUD	-4.41	0.48	-10.90	-4.64	-3.43	73.79	-5.10	-3.95	77.57
CAD	-7.62	-3.40	44.62	-5.12	-5.55	108.27	-5.02	-4.32	86.10
CHF	-1.86	-0.35	18.64	-1.48	-0.66	44.26	-1.54	-0.79	51.64
DKK	-0.90	-1.07	119.00	-1.99	-1.46	73.20	-2.48	-1.55	62.24
EUR	-4.79	-1.03	21.47	-4.59	-2.14	46.64	-4.21	-2.19	52.04
GBP	-5.10	0.35	-6.90	-5.04	-1.87	37.12	-5.06	-2.25	44.47
JPY	-3.75	-0.00	0.05	-3.20	0.10	-3.10	-3.96	-0.19	4.79
NOK	2.15	0.12	5.70	1.15	0.14	12.24	0.73	-0.06	-8.28
NZD	3.21	0.85	26.36	-0.01	-0.98	7839.90	-1.08	-2.68	248.03
SEK	-3.08	0.45	-14.74	-2.63	-1.60	61.00	-3.21	-1.71	53.27
USD	-3.96	-7.08	178.80	-3.97	-4.19	105.59	-3.67	-3.78	103.11

Notes: The table reports the cumulative changes in sovereign yields over all dates, the FOMC windows, and the ratio between the latter and the former. For each series, we compute the average values within the last year and the first year, and then compute the difference.

Table 3: Factor structure of ∇y_t.

	AUD	CAD	CHF	DKK	EUR	GBP	JPY	NOK	NZD	SEK	USD
3m	0.06	0.10	0.02	-0.11	0.03	0.04	-0.05	0.13	0.14	0.09	0.12
6m	0.06	0.10	0.04	-0.02	0.04	0.06	0.00	0.10	0.06	0.05	0.10
1y	0.07	0.10	0.07	0.05	0.07	0.08	0.05	0.06	0.03	0.05	0.08
2y	0.09	0.09	0.10	0.10	0.09	0.09	0.06	0.02	0.06	0.09	0.07
3y	0.09	0.09	0.11	0.11	0.09	0.08	0.07	0.02	0.07	0.09	0.07
4y	0.08	0.09	0.10	0.12	0.09	0.09	0.09	0.04	0.08	0.09	0.08
5y	0.09	0.08	0.10	0.12	0.09	0.09	0.11	0.06	0.08	0.08	0.08
6y	0.09	0.08	0.09	0.12	0.10	0.10	0.13	0.09	0.09	0.09	0.08
7y	0.10	0.07	0.09	0.13	0.10	0.10	0.14	0.11	0.09	0.09	0.08
8y	0.10	0.07	0.09	0.13	0.10	0.10	0.14	0.12	0.10	0.10	0.08
9y	0.10	0.07	0.09	0.13	0.10	0.09	0.13	0.13	0.10	0.10	0.08
10y	0.08	0.06	0.09	0.11	0.08	0.07	0.12	0.12	0.10	0.08	0.08
% Var.	83	98	90	95	97	93	82	85	89	81	98

Notes: Each column reports the weights on sovereign yields for ∇y_t, the first principal component of cumulative changes in sovereign yields during the three-day FOMC windows. The data frequency is monthly.

where $y_t^{(n)}$ is the n-year sovereign yield, $\boldsymbol{\tau}_t$ is a vector of proxies for the trend. The equation is estimated for each country separately. For each country except the U.S., we let

$$\boldsymbol{\tau}_t = \begin{bmatrix} \nabla y_{loc,t} & \nabla y_{US,t} \end{bmatrix}^\top,$$

where $\nabla y_{loc,t}$ is the first principal component of changes in sovereign yields during the three-day windows around FOMC announcements, and $\nabla y_{US,t}$ is analogously defined for U.S. Treasury yields. We include the 3-month, 6-month, and 1-year through 10-year maturities for computing the principal components. For the U.S., $\boldsymbol{\tau}_t = \nabla y_{US,t}$. Following Stock and Watson (1993), we include leads and lags of the first-differenced $y_t^{(n)}$ and $\boldsymbol{\tau}_t$ in the regression to estimate β_0 and $\boldsymbol{\gamma}$. We focus on the 10-year yield as the dependent variable and choose four leads and lags. The data are monthly and range from January 1990 to December 2022, with some countries starting at later dates.

Table 4 reports the estimates of β_0 and $\boldsymbol{\gamma}$ as well as persistence test statistics for the cointegration residuals $\hat{u}_t = y_t^{(n)} - \hat{\beta}_0 - \hat{\boldsymbol{\gamma}}^\top \boldsymbol{\tau}_t$. The standard errors for the regression coefficients are Newey-West with six lags. The persistence properties of the residuals are highly

consistent across countries: the Augmented Dickey-Fuller (ADF) and Phillips-Perron (PP) tests reject the unit root hypothesis at highly significant levels, and the Müller and Watson (2013) low-frequency stationary test (LFST) fails to reject stationarity.

It is interesting to investigate the values of $\boldsymbol{\gamma}$. The value 1 is within one standard deviation away from the point estimate $\hat{\gamma}_{loc}$ or $\hat{\gamma}_{US}$ for most countries, implying that the long-run trend of the country's sovereign yields moves one-for-one with the cumulative effects of U.S. monetary policy. For Canada (CAD), Switzerland (CHF), U.K. (GBP), Japan (JPY), and Norway (NOK), the coefficient on $\nabla y_{US,t}$ is larger than that on $\nabla y_{loc,t}$; and the coefficients on $\nabla y_{loc,t}$ are even negative for the U.K., Japan, and Norway, implying that the trends of these countries' sovereign yields are mainly driven by changes in *U.S.* interest rates instead of their own interest rates during FOMC announcement windows. This strengthens the fact that U.S. monetary policy drives the persistent variations in global interest rates.

The regression results suggest that global sovereign yields are cointegrated with $\nabla y_{loc,t}$ and $\nabla y_{US,t}$, and the regression residuals are stationary. Motivated by this result, the last panel of Table 4 reports estimation results of an error-correction model

$$\Delta y_t^{(n)} = c + \alpha \hat{u}_{t-1} + A(L)\Delta y_t^{(n)} + B(L)\Delta \boldsymbol{\tau}_t + \varepsilon_t^{(n)}, \tag{3}$$

where $\Delta y_t^{(n)} = y_t^{(n)} - y_{t-1}^{(n)}$, $\hat{u}_{t-1}$ is the residual from Equation (2), $A(L)$ and $B(L)$ are polynomials of lag operators. The loadings of the differenced yield on the cointegrated variable (ECM $\hat{\alpha}$) are negative and statistically significant for all countries. It implies that the cumulative effects of U.S. monetary policy, $\boldsymbol{\tau}_t$, is informative about future sovereign yields. Whenever sovereign yields deviate from the trend implied by $\boldsymbol{\tau}_t$, future yields should revert to this trend. Next, we exploit this property in predictive regressions for excess bond returns.

3.3 Predicting Excess Bond Returns

3.3.1 Baseline Regression

The excess return for holding an n-year bond for a quarter is

$$rx_{t+3}^{(n)} = -(n - \frac{1}{4})y_{t+3}^{(n-\frac{1}{4})} + ny_t^{(n)} - \frac{1}{4}y_t^{(\frac{1}{4})}, \tag{4}$$

Table 4: Cointegration tests for the 10-year yield and macroeconomic trends.

	AUD	CAD	CHF	DKK	EUR	GBP	JPY	NOK	NZD	SEK	USD
constant	-2.06	-3.59	-3.69	-2.09	-4.61	0.38	-2.72	-6.93	-3.01	-4.33	-1.98
	(0.75)	(0.48)	(0.51)	(1.43)	(0.35)	(1.46)	(0.26)	(1.05)	(1.06)	(0.71)	(0.22)
$\nabla y_{loc,t}$	0.34	0.23	0.01	0.84	0.88	-0.75	-0.79	-1.79	1.12	0.86	1.36
	(0.37)	(0.16)	(0.31)	(0.29)	(0.34)	(0.27)	(0.19)	(0.40)	(0.48)	(0.43)	(0.05)
$\nabla y_{US,t}$	1.17	1.39	1.30	0.54	0.65	2.21	1.48	4.08	0.63	0.78	
	(0.39)	(0.16)	(0.29)	(0.57)	(0.47)	(0.21)	(0.15)	(0.47)	(0.35)	(0.65)	
R^2	0.81	0.92	0.92	0.90	0.93	0.90	0.87	0.93	0.79	0.87	0.93
SD	0.98	0.72	0.67	0.88	0.77	0.78	0.63	0.79	0.90	1.19	0.50
$\hat{\rho}$	0.96	0.94	0.96	0.96	0.96	0.94	0.93	0.89	0.94	0.98	0.88
Half-life	15.9	11.7	16.2	17.5	16.3	11.5	9.9	6.0	12.1	27.5	5.4
ADF	-3.18**	-3.26**	-2.59*	-3.10**	-2.75*	-3.30**	-2.75*	-3.64***	-3.08**	-3.01**	-5.17***
PP	-17.82**	-22.30***	-13.14*	-15.26**	-15.20**	-22.70***	-18.94**	-20.07**	-19.37**	-9.44	-50.07***
LFST	0.47	0.62	0.75	0.66	0.71	0.53	0.70	0.18	0.60	0.46	0.91
Johansen $r = 0$	33.01*	36.23**	33.69*	34.76*	30.94	28.21	35.10**	27.48	24.53	38.09**	30.09***
Johansen $r = 1$	16.39	14.84	17.65	18.39*	15.54	12.03	18.42*	12.80	12.26	15.53	8.27*
ECM $\hat{\alpha}$	-0.05	-0.05	-0.04	-0.06	-0.04	-0.03	-0.01	-0.04	-0.05	-0.06	-0.16
	(0.02)	(0.02)	(0.02)	(0.02)	(0.02)	(0.02)	(0.02)	(0.03)	(0.02)	(0.01)	(0.04)

Notes: * $p < 0.1$, ** $p < 0.05$, *** $p < 0.01$. Dynamic OLS regressions of the 10-year sovereign yield on average changes in domestic sovereign yields across all maturities during the three-day FOMC announcement windows. Newey-West standard errors with 6 lags are in parentheses. ∇y_t is the first principal component of cumulative changes in all sovereign yields of country i during FOMC windows. The second panel reports statistics for the cointegration residuals $\hat{u}_t = y_t^{(10)} - \hat{\beta}_0 - \hat{\boldsymbol{\gamma}}\boldsymbol{\tau}_t$, including standard deviations (SD), first-order autocorrelation coefficients ($\hat{\rho}$), half-lives ($\ln(0.5)/\ln(\hat{\rho})$), Augmented Dickey-Fuller (ADF) and Phillips-Perron (PP) unit root test statistics, and p-values for Müller-Watson low-frequency stationary test (LFST). The third panel reports the Johansen trace statistic for the cointegration rank (r) among the sovereign yields and $\boldsymbol{\tau}_t$ against the alternative that the rank exceeds the specified level. It also reports estimates of α for an error-correction model $\Delta y_t^{(n)} = c + \alpha\hat{u}_{t-1} + A(L)\Delta y_t^{(n)} + B(L)\Delta\boldsymbol{\tau}_t + \varepsilon_t^{(n)}$.

where n indicates maturity in years and t indicates monthly time.

We estimate the regression for each country i at the monthly frequency:

$$\overline{rx}_{t+3} = \beta_0 + \boldsymbol{\beta}_1^\top \boldsymbol{PC}_t + \boldsymbol{\gamma}^\top \boldsymbol{\tau_t} + \varepsilon_{t+3}, \tag{5}$$

where $\overline{rx}_{t+3} = \frac{1}{10}\sum_{n=1}^{10} rx_{t+3}^{(n)}$ is the average excess bond return over the quarterly holding period, $\boldsymbol{PC}_t$ is the first three principal components of country i's sovereign yield curve. Our benchmark is the $\boldsymbol{PC}_t$-only model, which only uses the principal components of the current yields to predict excess bond returns. If the *spanning hypothesis* holds, the state variables determining the yield curve can be expressed as linear combinations of current yields, and thus, the principal components contain all information for predicting bond returns. A significant coefficient on $\boldsymbol{\tau_t}$ rejects the spanning hypothesis. We specify $\boldsymbol{\tau_t}$ from the following list one by one: (1) the country's inflation trend[2] (π_t^*), (2) the first principal component of cumulative changes in the country's sovereign yields during the three days around the U.S. FOMC announcement dates ($\nabla y_{loc,t}$); (3) the first principal component of cumulative changes in U.S. yields during the FOMC announcement windows ($\nabla y_{US,t}$); (4) $\nabla y_{loc,t}$ and $\nabla y_{US,t}$.

Table 5 reports the predictive regression results for G10 sovereign excess bond returns. Adding trend inflation to the regression only marginally improves the R^2. The FOMC factors, on the contrary, substantially increase the R^2 for all countries. Compared with the $\boldsymbol{PC}_t$-only model, adding the cumulative effects of FOMC announcements on the sovereign or U.S. yield curve at least doubles the R^2 and can even quadruples the R^2 for Germany, New Zealand, Norway, and the U.S.

The coefficient γ is also significant for $\nabla y_{loc,t}$ or $\nabla y_{US,t}$. We report the Newey-West standard error and the small-sample p-value using the bootstrap method of Bauer and Hamilton (2018). Except for Australia and Norway, at least one coefficient on $\nabla y_{loc,t}$ or $\nabla y_{US,t}$ has a p-value below 10% for each country. For Australia and Norway, the t-statistics for the coefficient on $\nabla y_{loc,t}$ have absolute values over 3 in Specification (2). The coefficients are negative,

[2]The construction of π_t^* follows Cieslak and Povala (2015): $\pi_t^* = (1-\nu)\sum_{s=0}^{t-1} \nu^s \pi_{t-s}^{yoy}$, where π_{t-s}^{yoy} is the monthly percentage change in CPI relative to the same month of the previous year. We truncate the sum at 120 months and set $\nu = 0.987$. The inflation data are from OECD's Monthly Economic Indicators. For Australia and New Zealand, we only have quarterly data that matches the time span of the interest rates. We linearly interpolate the quarterly π_t^{yoy} to the monthly frequency and then compute the trend inflation series.

implying that when current yields are above the FOMC trend ($\boldsymbol{\tau}_t$ decreases), future yields are expected to decrease, and bond returns will increase.

Next, we investigate why including $\boldsymbol{\tau}_t$ as predictors increases predictive power. We estimate two sets of regressions using orthogonalized predictors. First, we orthogonalize the yields with $\boldsymbol{\tau}_t$ and use the residuals to predict excess bond returns. Second, we orthogonalize $\boldsymbol{\tau}_t$ with the yields and use the residuals to predict excess bond returns. By the Frisch-Waugh-Lovell theorem, the slope coefficients from these regressions should correspond[3] to $\boldsymbol{\beta}_1$ and $\boldsymbol{\gamma}$ in Equation (5), so we are not interested in the slope coefficients for these regressions. Instead, we focus on the R^2.

3.3.2 Orthogonalzied Yields

The cointegration analysis implies that the deviations of yields from $\boldsymbol{\tau}_t$ are informative about future yields. Here, we investigate the predictive power of the cointegration residuals for excess bond returns. We estimate the following regression for each country i:

$$\overline{rx}_{t+3} = \beta_0 + \boldsymbol{\beta}_1^\top \widetilde{\boldsymbol{PC}}_t + \varepsilon_{t+3}, \tag{6}$$

where $\widetilde{\boldsymbol{PC}}_t$ denotes the first three principal components of orthogonalized yields, which are the residuals from regressing country i's sovereign yields on $\boldsymbol{\tau}_t$. Note that we first orthogonalize all the yields and then take the principal components, so $\widetilde{\boldsymbol{PC}}_t$ is distinct from the orthogonalized $\boldsymbol{PC}_t$, as it captures the summarized information of all the orthogonalized yields, rather than solely the orthogonalized three principal components. The specifications of $\boldsymbol{\tau}_t$ are the same as in the baseline regression: (1) π_t^*, (2) $\nabla y_{loc,t}^{FOMC}$, (3) $\nabla y_{US,t}^{FOMC}$, and (4) $\nabla y_{loc,t}^{FOMC}$ & $\nabla y_{US,t}^{FOMC}$.

We also consider two other specifications of $\widetilde{\boldsymbol{PC}}_t$: the first three principal components of cumulative changes in country i's sovereign yields or U.S. Treasury yields outside the FOMC windows. The specification is motivated by the fact that

$$1 = \mathbf{1}_{FOMC}(s) + \mathbf{1}_{nonFOMC}(s), \quad \forall s, \tag{7}$$

[3]They are not equal because we use a subset of principal components of the yields in Equation (5), but we orthogonalized $\boldsymbol{\tau}_t$ with the full set of yields, and orthogonalize the full set of yields with $\boldsymbol{\tau}_t$. Notwithstanding, the slope coefficients from the orthogonalized regressions are very similar to those from Equation (5).

Table 5: Predictive Regressions for Excess Bond Returns

		AUD	CAD	CHF	DKK	EUR	GBP	JPY	NOK	NZD	SEK	USD
PC	R^2	0.03	0.07	0.07	0.08	0.03	0.04	0.13	0.06	0.04	0.03	0.04
π_t^*	γ	0.36	-0.32	-0.49	-2.40	-0.29	-0.17	-0.37	8.72	-1.37	-0.44	-1.95
	SD	(0.72)	(0.61)	(0.47)	(1.49)	(0.78)	(0.41)	(0.36)	(2.59)	(1.20)	(0.82)	(0.81)
	p-val	[0.87]	[0.86]	[0.64]	[0.56]	[0.92]	[0.91]	[0.64]	[0.44]	[0.88]	[0.83]	[0.27]
	R^2	0.04	0.08	0.08	0.11	0.03	0.04	0.13	0.29	0.06	0.04	0.08
$\nabla y_{loc,t}$	γ	-1.34	-0.70	-1.47	-0.96	-1.57	-2.40	-0.65	-6.62	-6.77	-0.53	-2.22
	SD	(0.43)	(0.44)	(0.33)	(0.32)	(0.40)	(0.71)	(0.28)	(2.00)	(1.75)	(0.43)	(0.42)
	p-val	[0.14]	[0.52]	[0.01]	[0.12]	[0.03]	[0.06]	[0.18]	[0.46]	[0.02]	[0.81]	[0.00]
	R^2	0.10	0.09	0.21	0.15	0.16	0.16	0.17	0.22	0.22	0.05	0.17
$\nabla y_{US,t}$	γ	-0.74	-1.63	-1.07	-1.35	-1.39	-2.83	-0.63	-2.25	-1.52	-0.87	-2.22
	SD	(0.29)	(0.40)	(0.28)	(0.43)	(0.39)	(0.71)	(0.23)	(1.47)	(1.05)	(0.43)	(0.42)
	p-val	[0.24]	[0.02]	[0.03]	[0.08]	[0.06]	[0.03]	[0.11]	[0.84]	[0.34]	[0.40]	[0.00]
	R^2	0.08	0.15	0.19	0.16	0.13	0.19	0.18	0.08	0.07	0.07	0.17
$\nabla y_{loc,t}$	γ	-1.30	-0.30	-1.27	-0.29	-1.36	-0.92	-0.14	-9.26	-8.85	0.64	
	SD	(0.66)	(0.44)	(0.61)	(0.61)	(0.65)	(0.75)	(0.46)	(3.13)	(2.90)	(1.25)	
	p-val	[0.23]	[0.82]	[0.12]	[0.74]	[0.14]	[0.38]	[0.84]	[0.10]	[0.05]	[0.72]	
$\nabla y_{US,t}$	γ	0.10	0.15	0.21	0.16	0.16	0.20	0.18	0.24	0.24	0.07	
	SD	(0.66)	(0.44)	(0.61)	(0.61)	(0.65)	(0.75)	(0.46)	(3.13)	(2.90)	(1.25)	
	p-val	[0.96]	[0.05]	[0.80]	[0.37]	[0.79]	[0.09]	[0.40]	[0.41]	[0.42]	[0.46]	
	R^2	0.10	0.15	0.21	0.16	0.16	0.20	0.18	0.24	0.24	0.07	

Notes: The first panel reports the R^2 from the $\boldsymbol{PC}_t$-only model. The remaining panels report the results of the regression $\overline{rx}_{t+3} = \beta_0 + \boldsymbol{\beta}_1^\top \boldsymbol{PC}_t + \gamma\tau_t + \varepsilon_{t+3}$, and the first column identifies τ_t. Each panel reports the point estimate of γ, its Newey-West standard error in parentheses, its small-sample p-value à la Bauer and Hamilton (2018) in brackets, and the R^2 of the regression. $\boldsymbol{PC}_t$: the first three principal components of the sovereign yield curve. CP: the Cochrane-Piazzesi factor for the sovereign yields. $\nabla y_{loc,t}$ and $\nabla y_{US,t}$: the first principal component of cumulative changes in domestic and U.S. yields during the 3-day FOMC windows.

and thus, any time series can be decomposed as the sum of cumulative changes during the two disjoint sets of dates. We interpret $\widetilde{\boldsymbol{PC}}_t$ as the yields' deviation from the cointegration trend, and analogously, $\nabla y_{loc,t}^{(n),nonFOMC}$ can also be interpreted as the yield's deviation from the FOMC trend. We explore whether the simple decomposition gives good approximates to the cointegration residuals in predicting excess bond returns.

Table 6 reports the R^2 of regression Equation (6). The first panel replicates the R^2 of the $\boldsymbol{PC}_t$-only regression in Table 5. The second panel reports the R^2 from the regressions using orthogonalized yields. The yields orthogonalized by $\nabla y_{loc,t}$ or $\nabla y_{US,t}$ produce substantially larger R^2 than the original yields, similar to those reported in Table 5. Orthogonalizing with $\nabla y_{loc,t}^{FOMC}$ or $\nabla y_{US,t}^{FOMC}$ (individually) appears to result in similar R^2 for each country except Norway and New Zealand, for which orthogonalizing with domestic $\nabla y_{loc,t}^{FOMC}$ results in substantially a larger R^2. The similar effects of $\nabla y_{loc,t}^{FOMC}$ and $\nabla y_{US,t}^{FOMC}$ are because world interest rates are synchronized with the U.S. Treasury yields during FOMC announcement windows, as shown in Figure 1. Accordingly, the persistent variations in world nominal interest rates are primarily determined by their common responses to U.S. monetary policy announcements.

The principal components of $\nabla y_{loc,t}^{nonFOMC}$ or $\nabla y_{US,t}^{nonFOMC}$ also produce much larger R^2 than the principal components of observed yields, with similar magnitudes to the R^2 produced by cointegration residuals. As shown in Figure 1, the yields outside FOMC windows are almost stationary. Therefore, $\nabla y_{loc,t}^{nonFOMC}$ plays a similar role as the cointegration error: pulling the interest rates towards the FOMC trend. For Switzerland, Denmark, Germany, the U.K., Japan, and Sweden, the domestic $\nabla y_{loc,t}^{nonFOMC}$ series produce larger R^2s than the U.S. $\nabla y_{US,t}^{nonFOMC}$ series, which is intuitive. The cointegration trends for the sovereign yields are determined by U.S. monetary policy announcements, but the reversions towards the trend are country-specific.

3.3.3 Orthogonalized $\boldsymbol{\tau}_t$

Next, we investigate whether $\boldsymbol{\tau}_t$ contains information on term premia. We orthogonalize $\boldsymbol{\tau}_t$ with sovereign yields of country i and use the residual $\widetilde{\boldsymbol{\tau}}_t$ to predict excess bond returns:

$$\overline{rx}_{t+3} = \beta_0 + \boldsymbol{\gamma}^\top \widetilde{\boldsymbol{\tau}}_t + \varepsilon_{t+3}. \tag{8}$$

Table 6: Predictive R^2 for excess bond returns: orthogonalized yields.

	AUD	CAD	CHF	DKK	EUR	GBP	JPY	NOK	NZD	SEK	USD
PC	0.03	0.07	0.07	0.08	0.03	0.04	0.13	0.06	0.04	0.03	0.04
$\pi^*_{i,t}$	0.03	0.08	0.07	0.10	0.02	0.03	0.09	0.27	0.06	0.03	0.07
$\nabla y^{FOMC}_{loc,t}$	0.10	0.09	0.21	0.15	0.16	0.16	0.16	0.21	0.21	0.04	0.17
$\nabla y^{FOMC}_{US,t}$	0.08	0.15	0.19	0.16	0.13	0.19	0.15	0.07	0.06	0.06	0.17
$\nabla y^{FOMC}_{loc,t}$ & $\nabla y^{FOMC}_{US,t}$	0.09	0.15	0.18	0.16	0.16	0.19	0.12	0.20	0.23	0.05	
$\nabla y^{nonFOMC}_{loc,t}$	0.07	0.06	0.15	0.15	0.13	0.08	0.11	0.04	0.08	0.10	0.16
$\nabla y^{nonFOMC}_{US,t}$	0.11	0.09	0.05	0.07	0.06	0.04	0.11	0.08	0.12	0.03	0.16
$\nabla y^{nonFOMC}_{loc,t}$ & $\nabla y^{nonFOMC}_{US,t}$	0.13	0.13	0.18	0.16	0.15	0.14	0.20	0.22	0.22	0.14	

Notes: The first panel reports the R^2 from the $\boldsymbol{PC}_t$-only model. The second panel reports the R^2 of the regression $\overline{rx}_{t+3} = \beta_0 + \boldsymbol{\beta}_1^\top \widetilde{\boldsymbol{PC}}_t + \varepsilon_{t+3}$, and the first column identifies variable that produces $\widetilde{\boldsymbol{PC}}_t$. $\widetilde{\boldsymbol{PC}}_t$: the first three principal components of the residuals from regressing sovereign yields on $\boldsymbol{\tau}_t$. The third panel reports the R^2 of regressing excess bond returns on the first three principal components of cumulative changes in sovereign yields ($\nabla y^{nonFOMC}_{loc,t}$) or U.S. Treasury yields ($\nabla y^{nonFOMC}_{US,t}$) outside FOMC windows.

Here, $\widetilde{\boldsymbol{\tau}}_t$ is the residual from regressing $\boldsymbol{\tau}_t$ on the full set of sovereign yields of Country i instead of $\boldsymbol{PC}_t$ so that it is orthogonal to all current yields. Table 7 reports the R^2 from Equation (8). Cochrane and Piazzesi (2005) demonstrate that a linear combination of forward rates is a strong predictor of excess bond returns, and this factor contains information beyond the first three principal components of the yield curve. As $\widetilde{\tau}_t$ is a univariate predictor, we compare its predictive power with that of the Cochrane-Piazzesi factor. In our international sample, the country-specific Cochrane-Piazzesi factor achieves an R^2 in a univariate regression[4] similar to that obtained by the level, slope, and curvature factors for each country. This is consistent with the results in Cochrane and Piazzesi (2005) using U.S. data from 1964 to 2003. In contrast, the orthogonalized $\nabla y_{loc,t}^{FOMC}$ or $\nabla y_{US,t}^{FOMC}$ leads to a significantly larger predictive R^2 than the one achieved by $\boldsymbol{PC}_t$ or CP_t for most countries. Therefore, the cumulative effects of U.S. monetary policy announcements contain a wealth of information regarding bond risk premia, at least as informative as the currently observed yields.

In summary, the cumulative effects of U.S. monetary policy announcements on sovereign yields are the cointegration trends of world interest rates. They are informative of future yields and help predict excess bond returns. Since changes in expected yields are unpredictable[5], significant predictors for excess bond returns must capture fluctuations in the term premium. The substantial improvements in predictive power in Table 5 and Table 6 related to $\nabla y_{loc,t}^{FOMC}$ imply that U.S. monetary policy announcements capture the expectations hypothesis component of global yield curves. In our model, we show that the expected interest rates worldwide are indeed closely related to U.S. monetary policy.

4 Model

The model follows Bauer and Rudebusch (2020). We propose a new estimation method that avoids numerical optimization and speeds up the estimation. The estimation method allows for vector-valued trends for the state vector, and the scalar-τ_t model is a special case.

[4]The Cochrane-Piazzesi factor is $CP_t = \boldsymbol{\gamma}^\top \boldsymbol{f}_t$, where $\boldsymbol{f}_t = (y_t^{(1)}, f_t^{(1,1)}, f_t^{(2,1)}, \ldots, f_t^{(9,1)})^\top$ is a vector of the country's forward rates, and $\boldsymbol{\gamma}$ is estimated from $\overline{rx}_{t+3} = \beta_0 + \boldsymbol{\gamma}^\top \boldsymbol{f}_t + \varepsilon_{t+3}$. We estimate CP_t for each country individually.

[5]Under the expectations hypothesis, $rx_{t+1}^{(n)} = (\mathbf{E}_{t+1} - \mathbf{E}_t)\left[y_{t+1}^{(1)} + \cdots + y_{t+n-1}^{(1)}\right] + const.$ is orthogonal to time-t information.

Table 7: Predictive R^2 for excess bond returns: orthogonalized $\boldsymbol{\tau}_t$.

	AUD	CAD	CHF	DKK	EUR	GBP	JPY	NOK	NZD	SEK	USD
PC	0.03	0.07	0.07	0.08	0.03	0.04	0.13	0.06	0.04	0.03	0.04
CP_t	0.03	0.06	0.05	0.06	0.03	0.03	0.15	0.06	0.03	0.05	0.06
$\pi^*_{i,t}$	0.00	0.00	0.03	0.03	0.00	0.00	0.01	0.23	0.02	0.00	0.02
$\nabla y^{FOMC}_{loc,t}$	0.07	0.01	0.11	0.10	0.14	0.11	0.07	0.16	0.17	0.04	0.09
$\nabla y^{FOMC}_{US,t}$	0.05	0.07	0.10	0.09	0.11	0.16	0.07	0.04	0.03	0.07	0.09
$\nabla y^{FOMC}_{loc,t}$ & $\nabla y^{FOMC}_{US,t}$	0.07	0.07	0.11	0.10	0.14	0.17	0.08	0.16	0.19	0.08	

Notes: The first panel reports the R^2 from the $\boldsymbol{PC}_t$-only model and the univariate regression on the Cochrane-Piazzesi factor. The second panel reports the R^2 of the regression $\overline{rx}_{t+3} = \beta_0 + \boldsymbol{\gamma}^\top \widetilde{\boldsymbol{\tau}}_t + \varepsilon_{t+3}$. The first column identifies $\widetilde{\boldsymbol{\tau}}_t$, where $\widetilde{\boldsymbol{\tau}}_t$ denotes the residuals from regressing $\boldsymbol{\tau}_t$ on sovereign yields. $\nabla y^{FOMC}_{loc,t}$ ($\nabla y^{FOMC}_{loc,t}$): the first principal component of cumulative changes in sovereign (U.S.) yields during the FOMC windows.

The time unit for t and n in the model is one month. The model is estimated country by country, so the parameters are country-specific. To save notations, we ignore the country label i in the presentation of the model.

4.1 Model Setup

The state is a $K_X \times 1$ vector X_t, which evolves as

$$\begin{aligned} X_t =& \boldsymbol{\mu} + \Gamma \boldsymbol{\tau}_t + \tilde{X}_t, \\ \boldsymbol{\tau}_t =& \boldsymbol{\tau}_{t-1} + \boldsymbol{\eta}_t, \quad \boldsymbol{\eta}_t \sim \mathcal{N}(0, \Omega_\eta) \\ \tilde{X}_t =& \Phi \tilde{X}_{t-1} + \tilde{U}_t, \quad \tilde{U}_t \sim \mathcal{N}(0, \tilde{\Omega}), \end{aligned} \tag{9}$$

where $\boldsymbol{\tau}_t$ is a $K_\tau \times 1$ random walk and $\tilde{X}_t$ is a $K_X \times 1$ stationary VAR(1). The shocks are i.i.d over time and $\boldsymbol{\eta}_t \perp \tilde{U}_t$. Define

$$Z_t \equiv \begin{bmatrix} \boldsymbol{\tau}_t^\top & X_t^\top \end{bmatrix}^\top, U_t \equiv \Gamma \boldsymbol{\eta}_t + \tilde{U}_t, \Omega \equiv \mathbf{E}[U_t U_t^\top] = \Gamma \Omega_\eta \Gamma^\top + \tilde{\Omega}.$$

The log stochastic discount factor m_{t+1} evolves as

$$m_{t+1} = -\delta_0 - \boldsymbol{\delta}_1^\top X_t - \frac{1}{2} \Lambda_t^\top \Lambda_t - \Lambda_t^\top \Omega^{-\frac{1}{2}} U_{t+1}. \tag{10}$$

The price of risk is an affine function of Z_t:

$$\Lambda_t = \Omega^{-\frac{1}{2}} (\Lambda_0 + \Lambda_1 Z_t). \tag{11}$$

Note that the SDF is driven by a $K_X \times 1$ dimensional shock with the same dimension as X_t, but is a combination of shocks to $\boldsymbol{\tau}_t$ and $\tilde{X}_t$. Although the trend $\boldsymbol{\tau_t}$ does not directly affect the observed yields, it affects risk premia by affecting the price of risk. We assume that Λ_1 satisfies

$$\Lambda_1 = \begin{bmatrix} (I - \Phi)\Gamma, \Lambda_{12} \end{bmatrix}, \tag{12}$$

i.e., the first K_τ column of Λ_1 (the loading on $\boldsymbol{\tau}_t$) equals $(I - \Phi)\Gamma$ and the remaining K_X columns is an unrestricted $K_X \times K_X$ matrix Λ_{12}. It can be shown that the log zero-coupon

bond prices are affine in X_t:

$$p_t^{(n)} = \mathcal{A}_n + \mathcal{B}_n^\top X_t, \tag{13}$$

where $\mathcal{A}_n$ and $\mathcal{B}_n$ satisfy the usual no-arbitrage recursions:

$$\mathcal{A}_n = \mathcal{A}_{n-1} - \delta_0 + \mathcal{B}_{n-1}^\top (I - \Phi)\boldsymbol{\mu} + \frac{1}{2}\mathcal{B}_{n-1}^\top \Omega \mathcal{B}_{n-1} - \mathcal{B}_{n-1}^\top \Lambda_0, \tag{14}$$

$$\mathcal{B}_n^\top = -\boldsymbol{\delta}_1^\top + \mathcal{B}_{n-1}^\top (\Phi - \Lambda_{12}). \tag{15}$$

The initial values are $\mathcal{A}_0 = 0, \mathcal{B}_n = \mathbf{0}$. The yields are

$$y_t^{(n)} = A_n + B_n^\top X_t, \tag{16}$$

with $A_n = -\frac{1}{n}\mathcal{A}_n$ and $B_n = -\frac{1}{n}\mathcal{B}_n$.

The log risk-neutral bond prices solve

$$p_t^{(n),rn} = \ln \mathbf{E}_t \left[\exp \left\{ -y_t^{(1)} + p_{t+1}^{(n-1),rn} \right\} \right], \tag{17}$$

which is an affine function of X_t and $\boldsymbol{\tau}_t$:

$$p_t^{(n),rn} = \mathcal{A}_n^{rn} + \mathcal{B}_n^{rn\top} X_t + \mathcal{C}_n^{rn\top} \boldsymbol{\tau}_t \tag{18}$$

and the coefficients solve the recursions

$$\begin{aligned}
\mathcal{A}_n^{rn} =& \mathcal{A}_{n-1}^{rn} - \delta_0 + \mathcal{B}_{n-1}^{rn\top}(I - \Phi)\boldsymbol{\mu} + \frac{1}{2}\mathcal{B}_{n-1}^{rn\top}\Omega\mathcal{B}_{n-1}^{rn} \\
&+ \frac{1}{2}\left(\mathcal{B}_{n-1}^{rn\top}\Gamma\Omega_\eta\mathcal{C}_{n-1}^{rn} + \mathcal{C}_{n-1}^{rn\top}\Omega_\eta\Gamma^\top\mathcal{B}_{n-1}\right) + \frac{1}{2}\mathcal{C}_{n-1}^{rn\top}\Omega_\eta\mathcal{C}_{n-1}^{rn}, \\
\mathcal{B}_n^{rn\top} =& -\boldsymbol{\delta}_1^\top + \mathcal{B}_{n-1}^{rn\top}\Phi, \\
\mathcal{C}_n^{rn\top} =& \mathcal{B}_{n-1}^{rn\top}(I - \Phi)\Gamma + \mathcal{C}_{n-1}^{rn\top}
\end{aligned} \tag{19}$$

with $\mathcal{A}_0^{rn} = 0, \mathcal{B}_0^{rn} = \mathbf{0}, \mathcal{C}_0^{rn} = \mathbf{0}$. Clearly, risk-neutral rates explicitly depend on $\boldsymbol{\tau}_t$.

4.2 Estimation

For each country, we estimate the dynamic term structure model using two methods. Both methods treat X_t as observable and let it be the first five principal components of the $3, 4, \ldots, 120$-month yields following Adrian et al. (2013). The yields are interpolated using the Svensson (1994) parameters estimated from the yield curve data.

The first method assumes that τ_t is observable. Following Bauer and Rudebusch (2020), we label it the "observed shifting endpoint" (OSE) model. To investigate the role of monetary policy, our empirical proxy for $\boldsymbol{\tau}_t$ is $(\nabla y_{loc,t}, \nabla y_{US,t})^\top$, the first principal components of the cumulative daily changes in the cross-sections of domestic and U.S. zero-coupon yields during the three-day FOMC windows. For the U.S., $\boldsymbol{\tau}_t = \nabla y_{US,t}$. The results are quantitatively similar if we use changes during the FOMC window in individual yields, such as the 10-year yield. The previous sections have demonstrated that ∇y_t well accounts for the common trend of Treasury yields and contains essential information on expected yields and term premia. Therefore, ∇y_t is a good summary of the downward trend of the yield curve over the past three decades. Our baseline estimation uses monthly observations, taking the end-of-month values from our daily series of τ_t and the Treasury yields.

Given observed X_t and $\boldsymbol{\tau}_t$, we estimate the term structure model parameters using linear regressions à la Adrian et al. (2013). To account for τ and the unspanning-restriction (12), we modify the regression equations and run a restricted OLS. The Appendix presents details of the algorithm. The procedure selects a set of excess bond returns and regresses them on the state vector and the estimated shocks V_t. Following Adrian et al. (2013), we select excess bond returns of the one-month holding period for maturities $n \in \{6, 12, 18, 24, 30, 36, 42, 48, 54, 60, 84, 120\}$ months. The linear regression approach requires no numerical optimization algorithms, making it much faster than the OSE approach in Bauer and Rudebusch (2020).

The second method assumes that τ_t is unobservable. This approach uses only Treasury yields data and does not attribute the trend to any observed variables. Following Bauer and Rudebusch (2020), we label this approach the "estimated shifting endpoint" (ESE) model. Although the model does not explicitly recognize monetary policy as the driver of τ_t, the trends generated by the ESE model are quite similar to those generated by the OSE model using ∇y_t as the trend. We proceed in two steps. First, we estimate the parameters of the state process (9) and infer a scalar τ_t from observed X_t using the method in Del Negro et al. (2017b). Following Del Negro et al. (2017a) and Bauer and Rudebusch (2020), we specify a

tight inverse-gamma prior for Ω_η with a mean of $0.06^2/1200$, which implies that the standard deviation of the change in τ_t over a century is 6 percentage points. The Ω_η obtained from the $OSE : \nabla y_t$ model is about half of it. Our results are quantitatively similar if we use the value of Ω_η from the OSE model as the prior mean.

5 Trends and Term Premia of Forward Rates

The trend for the n-period yield in the model is defined as the long-term limit of its expectation:

$$y_t^{(n)*} \equiv \lim_{s\to\infty} \mathbf{E}_t \left[y_{t+s}^{(n)} \right] = A_n + B_n^\top \left(\boldsymbol{\mu} + \Gamma \boldsymbol{\tau}_t \right). \tag{20}$$

The n-by-m-period forward rate is

$$f_t^{(n,m)} = p_t^{(n)} - p_t^{(n+m)}, \tag{21}$$

and the n-by-m-period risk-neutral forward rate is

$$f_t^{(n,m),rn} = p_t^{(n),rn} - p_t^{(n+m),rn}, \tag{22}$$

which equals the sum of expected one-period yields between $t+n$ and $t+n+m$:

$$f_t^{(n,m),rn} = \mathbf{E}_t \left[y_{t+n}^{(1)} + y_{t+n+1}^{(1)} + \cdots + y_{t+n+m-1}^{(1)} \right] + const. \tag{23}$$

The term premium is

$$f_t^{(n,m),tp} = f_t^{(n,m)} - f_t^{(n,m),rn}. \tag{24}$$

Thanks to linearity, the trend for the forward rate is

$$f_t^{(n,m)*} \equiv \lim_{s\to\infty} \mathbf{E}_t \left[f_{t+s}^{(n,m)} \right] = -n y_t^{(n)*} + (n+m) y_t^{(n+m)*}. \tag{25}$$

By Equation (18) and Equation (20), the risk-neutral forward rate and the trend forward rate both directly load on the trend $\boldsymbol{\tau}_t$.

Following Wright (2011), we study the five-by-five-year forward rate. For each country, we plot the observed forward rate, its trend, and the term premium. We use two methods to

estimate the term premia. First, we are agnostic about the source and value of τ_t and estimate it from observed yields. This approach provides a robust estimation of τ_t, which we use as a benchmark. Second, we let the first principal component of changes in yields of all maturities during the three-day FOMC windows be the empirical proxies $\boldsymbol{\tau}_t = (\nabla y_{loc,t}, \nabla y_{US,t})^\top$, and use it to estimate model parameters.

5.1 Falling Stars

Figure 2 shows the forward rate trends for G10 countries. The five-by-five-year forward rates have declined substantially over the past three decades. Consistent with the observed persistent downward trends, our model also implies downward trending long-term expectations for G10 forward rates using τ_t inferred from observed yields. Although we use a scalar τ_t to summarize the trends in all yields for each country, the trends fit the observed interest rates very well.

The cumulative yield changes during U.S. monetary policy announcement windows serve as remarkably accurate proxies for world interest rate trends. Using the vector $(\nabla y_{loc,t}, \nabla y_{US,t})^\top$ as an empirical proxy for $\boldsymbol{\tau}_t$, our OSE method implies an $f_t^{(5,5)*}$ similar to that obtained by the ESE method. Except for Japan and Sweden, the OSE trends align well with observed interest rates and closely track the ESE trends. Although Japan and Sweden exhibited lower OSE trends compared to ESE trends before 2000, both methods indicate similar trends in the subsequent period. Our model demonstrates that yield changes during FOMC windows effectively capture global interest rate trends, successfully reproducing the stylized empirical facts.

We decompose the OSE trend into the contributions by local and U.S. responses to FOMC announcements according to

$$y_t^{(n)*} = A_n + B_n^\top (\boldsymbol{\mu} + \Gamma \boldsymbol{\tau}_t) = \left(A_n + B_n^\top \boldsymbol{\mu}\right) + B_n^\top \Gamma_{\cdot,1} \nabla y_{loc,t} + B_n^\top \Gamma_{\cdot,2} \nabla y_{US,t}, \tag{26}$$

and the forward rate trend $f_t^{(5,5)*}$ is determined according to Equation (25). In Figure 2, we plot forward trends associated with $B_n^\top \Gamma_{\cdot,1} \nabla y_{loc,t}$ and $B_n^\top \Gamma_{\cdot,2} \nabla y_{US,t}$, adjusting the initial values such that they coincide with that of the overall trend. For Australia, Canada, Switzerland, and the U.K., the secular declines in interest rates are mainly driven by $\nabla y_{US,t}$ instead of their own sovereign yields' responses to FOMC announcements. For the forward

rate trends of Denmark, Germany, New Zealand, and Sweden, the contributions by $\nabla y_{US,t}$ are almost flat. This is not because these countries' interest rates are independent of U.S. rates. The reality is quite the opposite: these countries' interest rates are highly synchronized with U.S. Treasury yields during FOMC announcement dates, so a single τ_t suffices for determining the interest rate trend.

In sum, long-term expectations of interest rates have been declining over the past three decades worldwide. This is in stark contrast to the implications of standard dynamic term structure models, which assume stationary state variables and thus imply constant limiting expectations. The shifting endpoint models suggest that the secular declines in world interest rates are primarily due to reductions in interest rate expectations. The cumulative effects of U.S. monetary policy announcements can well explain the worldwide variations in long-term expectations of interest rates.

5.2 Term Premium

Figure 3 displays the forward rate term premia for G10 countries. Two estimates of the term premium are shown for each country: (1) ESE, which utilizes inferred τ_t from observed yields, and (2) OSE, which employs the vector $(\nabla y_{loc,t}, \nabla y_{US,t})^\top$ as an empirical proxy for $\boldsymbol{\tau}_t$. Notably, the term premia implied by both methods are nearly identical. Stationary affine term structure models attribute the secular declines in interest rates primarily to reductions in term premia (for example, Wright (2011)) because the short-rate expectations converge to a constant at long horizons. In contrast, our ESE and OSE models indicate that term premia in developed economies, with the exception of Japan, appear to be stationary. The decline in world interest rates over time is primarily driven by decreases in expected short-term interest rates. This finding aligns well with the steady decline in policy rates observed over the past three decades, making it a more plausible outcome.

In a seminal paper, Wright (2011) estimates dynamic term structure models for G10 sovereign yields using GDP growth and inflation as macroeconomic state variables. His findings suggest significant declines in international term premia since 1990. Bauer et al. (2014) highlight the importance of correcting for small-sample bias when estimating state process parameters, but both papers assume a stationary VAR(1) process for the state vector, making them fixed-endpoint (FE) models. We extend the sample of Wright (2011)

Figure 2: Five-by-five-year forward rates and trends.

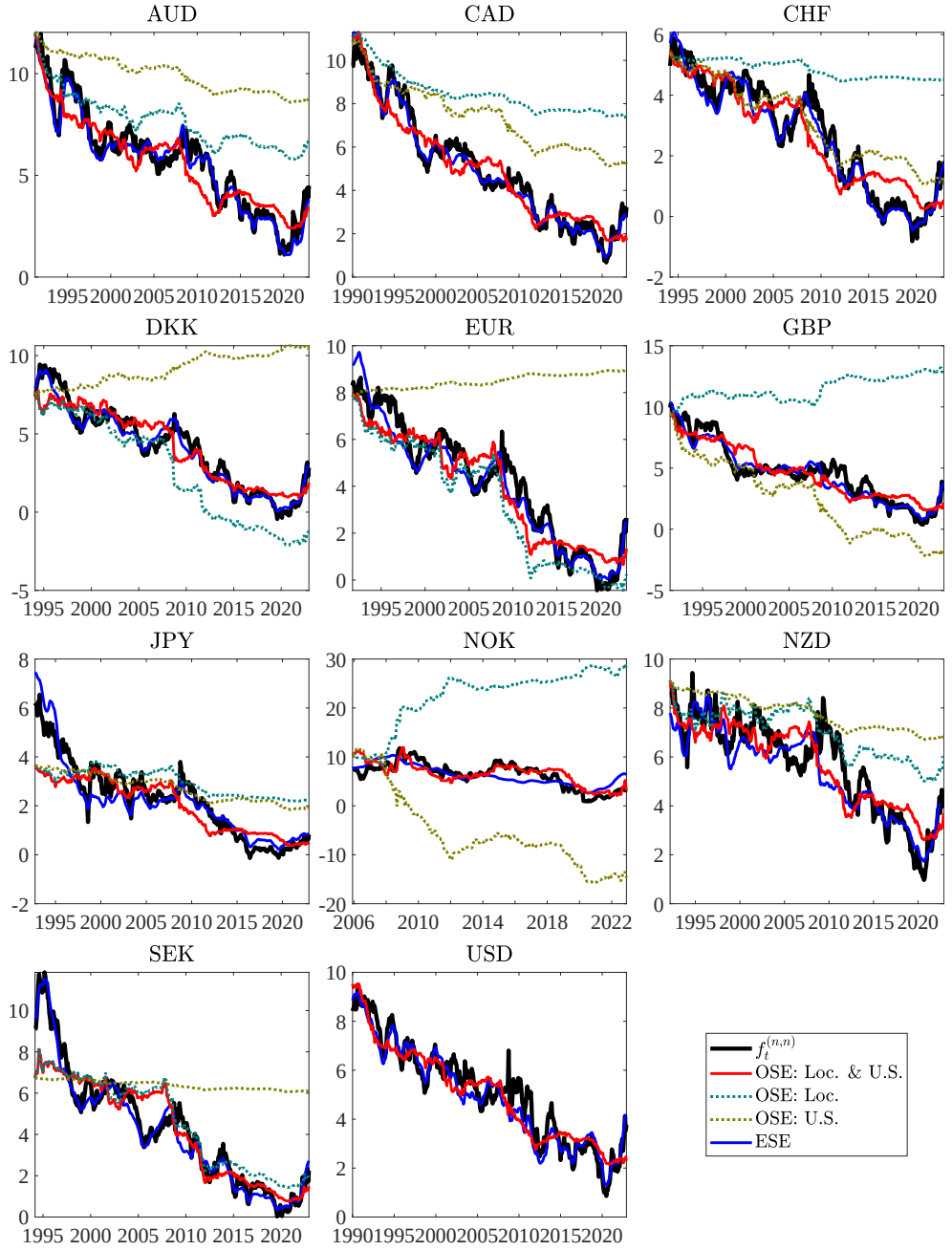

Notes: $f_t^{(n,n)}$: observed five-by-five-year forward rate. ESE: $f_t^{(5,5)*}$ implied by the ESE model. OSE: Loc. & U.S.: trend for the forward rate implied by the OSE model using two proxies for the persistent state: $\boldsymbol{\tau}_t = (\nabla y_{loc,t}, \nabla y_{US,t})^\top$, where $\nabla y_{loc,t}$ is the PC1 of cumulative changes in domestic sovereign yields during the FOMC windows, $\nabla y_{US,t}$ is the analog for U.S. Treasury yields. OSE: U.S. and OSE: Loc. are contributions of each proxy to the overall trend. The units are annualized percentage points.

Figure 3: Five-by-five-year forward rates and term premia.

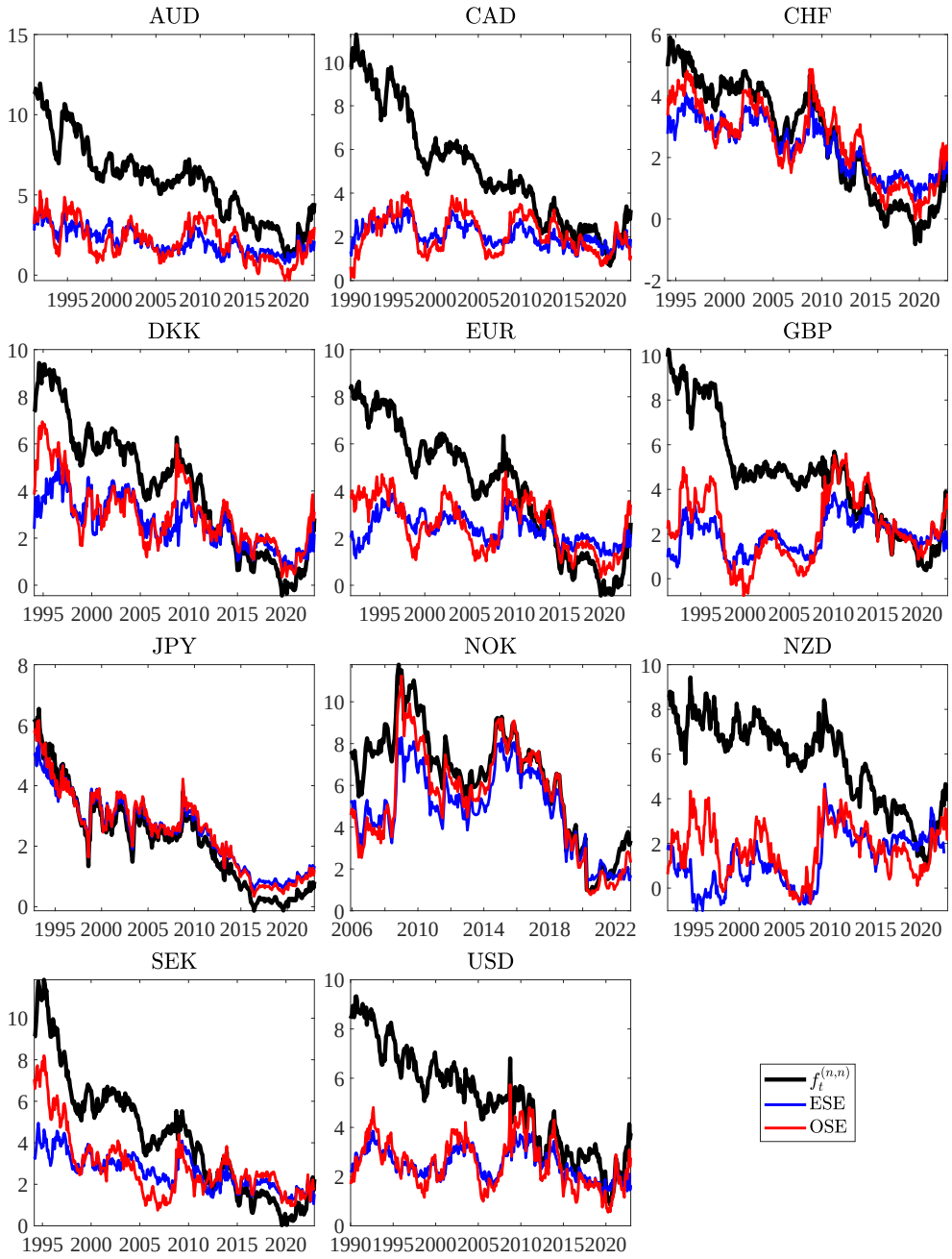

Notes: $f_t^{(n,n)}$: observed five-by-five-year forward rate. ESE: the term premium of the forward rate implied by the ESE model. OSE: the term premium of the forward rate implied by the OSE model, using two proxies for the persistent state: $\boldsymbol{\tau}_t = (\nabla y_{loc,t}, \nabla y_{US,t})^\top$, where $\nabla y_{loc,t}$ is the PC1 of cumulative changes in domestic sovereign yields during the FOMC windows, $\nabla y_{US,t}$ is the analog for U.S. Treasury yields. The maturities for computing the PC are the 3-month, 6-month, and 1-through-10-year maturities.

and Bauer et al. (2014). We compare their estimated term premia with those implied by our shifting-endpoint model. The quarterly sample spans from 1990Q1 to 2022Q4, except for Norway (1998Q1 to 2022Q4) and Sweden (1992Q4 to 2022Q4).

Figure 4 displays the five-by-five-year forward rates and the term premia obtained from different term structure models. The shifting-endpoint model is estimated using the ESE method. Bauer et al. (2014) stress that the bias-corrected term premia are countercyclical and demonstrate a less pronounced downward trend than Wright (2011). Our shifting-endpoint model implies significantly larger cyclical fluctuations in the term premia. Notably, the ESE model indicates spikes in term premia worldwide during the Global Financial Crisis, whereas the other two models do not imply such a phenomenon. Additionally, our shifting-endpoint model implies more stationary term premia. For instance, the term premia for Australia calculated by Bauer et al. (2014) and Wright (2011) declined by 5.6 and 9 percentage points, respectively, over the sample period. The ESE model, in contrast, suggests a relatively flat trend for the term premium.

6 U.S. Monetary Policy Announcements and Global Term Premia

6.1 Dynamics During FOMC Windows

Following the high-frequency monetary policy shock literature, we study the effects of U.S. monetary policy announcements on global short-rate expectations and term premia. Specifically, we analyze the cumulative changes in these components over the three-day FOMC windows. To this end, we apply the filter defined by Equation (1) to the 10-year risk-neutral rates and term premia to investigate their cumulative changes over the respective periods.

The risk-neutral rates and term premia are implied by an OSE model, where $(\nabla y_{loc,t}, \nabla y_{US,t})^\top$ serves as an observable proxy for $\boldsymbol{\tau}_t$. To facilitate the high-frequency analysis, we estimate the model parameters on a daily basis. We follow the procedures in Adrian et al. (2013) to get daily estimates. First, we estimate the model parameters using end-of-month data. Second, we compute the principal components of the daily yield curve, X_t, using weights computed from monthly data. Third, we combine the parameters estimated from monthly

Figure 4: Five-by-five-year forward rates and term premia: SE vs. FE.

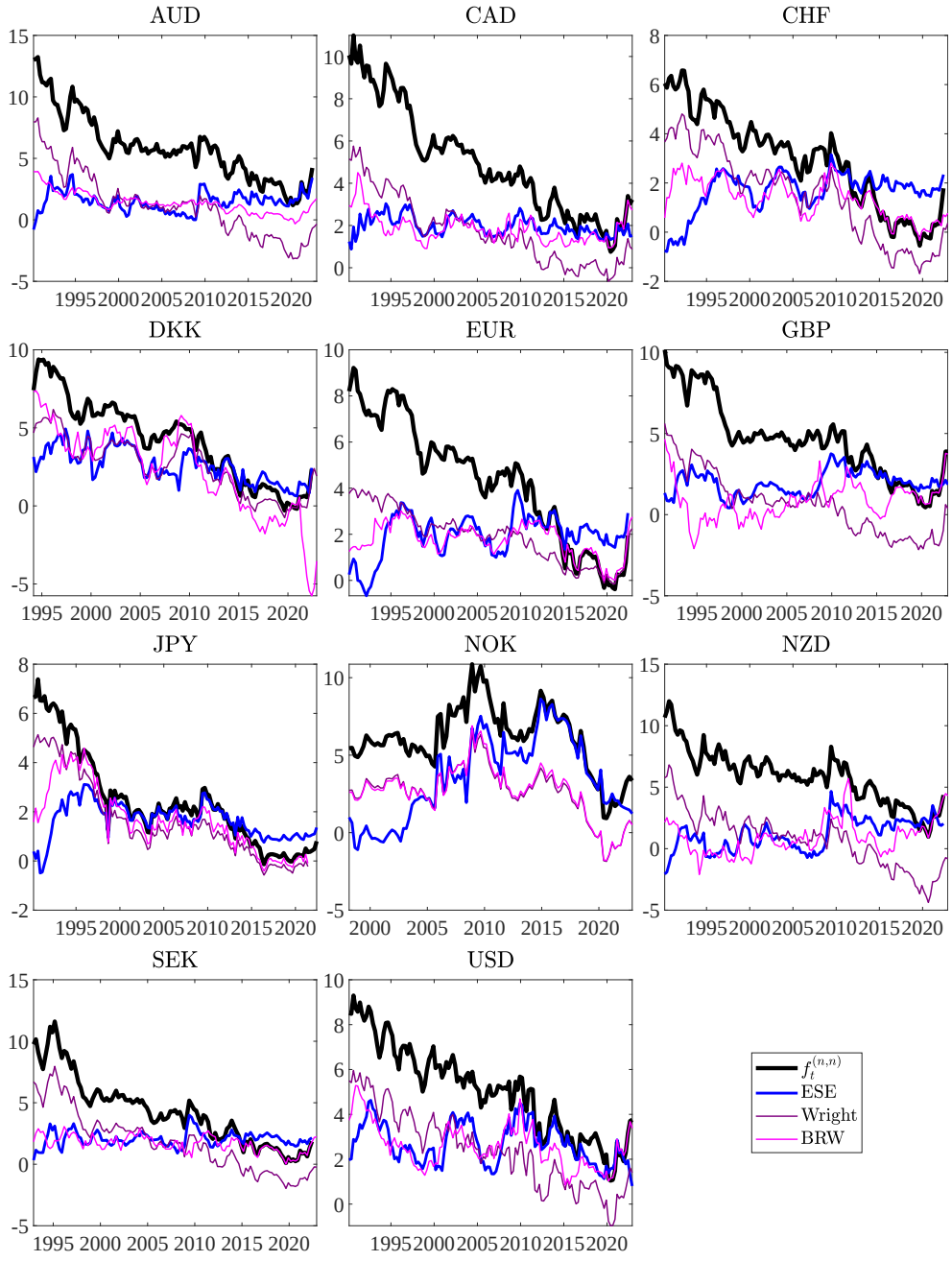

Notes: $f_t^{(n,n)}$: observed five-by-five-year forward rate. ESE: the term premium of the forward rate implied by the ESE model. Wright: the term premium estimated by Wright (2011). BRW: the term premium estimated by Bauer et al. (2014) using bias corrections for the state process parameters.

data with daily X_t and $\boldsymbol{\tau}_t$ to get the daily risk-neutral rates and term premia.

Short-rate expectations are crucial for monetary policy transmission in standard New Keynesian models. The expectations hypothesis holds in linear new Keynesian models and the responses of long-term interest rates to monetary policy shocks are all due to the responses of risk-neutral rates. Using the OSE model, we investigate the cumulative responses of global risk-neutral rates to U.S. monetary policy announcements during the FOMC windows. Figure 5 illustrates the 5-by-5-year forward risk-neutral rate and its cumulative changes, either within or outside the three-day FOMC windows, for each country. Since 1990, the U.S. risk-neutral rate has experienced a decline of 5.8 percentage points, with 5.7 percentage points of this decrease occurring specifically during the FOMC windows. Outside the FOMC window, the risk-neutral rate appears to remain relatively stable. For other countries, the fluctuations in risk-neutral rates are also remarkably concentrated in the FOMC windows and almost constant outside the FOMC windows.

Figure 6 depicts the 5-by-5-year forward term premia, exhibiting more pronounced cyclical fluctuations than risk-neutral yields. FOMC announcement dates have distinct effects on term premia and risk-neutral rates. The cumulative changes in term premia during FOMC announcement windows show a poorer fit to the observed series than risk-neutral rates, and the non-FOMC announcement dates are mainly responsible for fluctuations in term premia.

In summary, our analysis reveals a significant impact of U.S. monetary policy announcements on global interest rates. Short-rate expectations across the world are primarily shaped by these announcements, consistent with the standard transmission mechanism in New Keynesian models. In contrast, term premia appear to be influenced by a broader range of factors beyond just U.S. monetary policy. An interesting distinction between the term premia factors and U.S. monetary policy is that the former appears stationary while the latter exhibits a persistent downward trend.

6.2 The Importance of Shifting Endpoints

The significance of shifting endpoints extends beyond estimating expected interest rates and comprehending the persistent decline in interest rates. It also plays a pivotal role in estimating the impact of monetary policy on risk-neutral rates and term premia. Existing studies of monetary policy transmission rely on fixed-endpoint models (FE) to decompose

Figure 5: FOMC announcement dates and 5-by-5-year forward risk-neutral ratess.

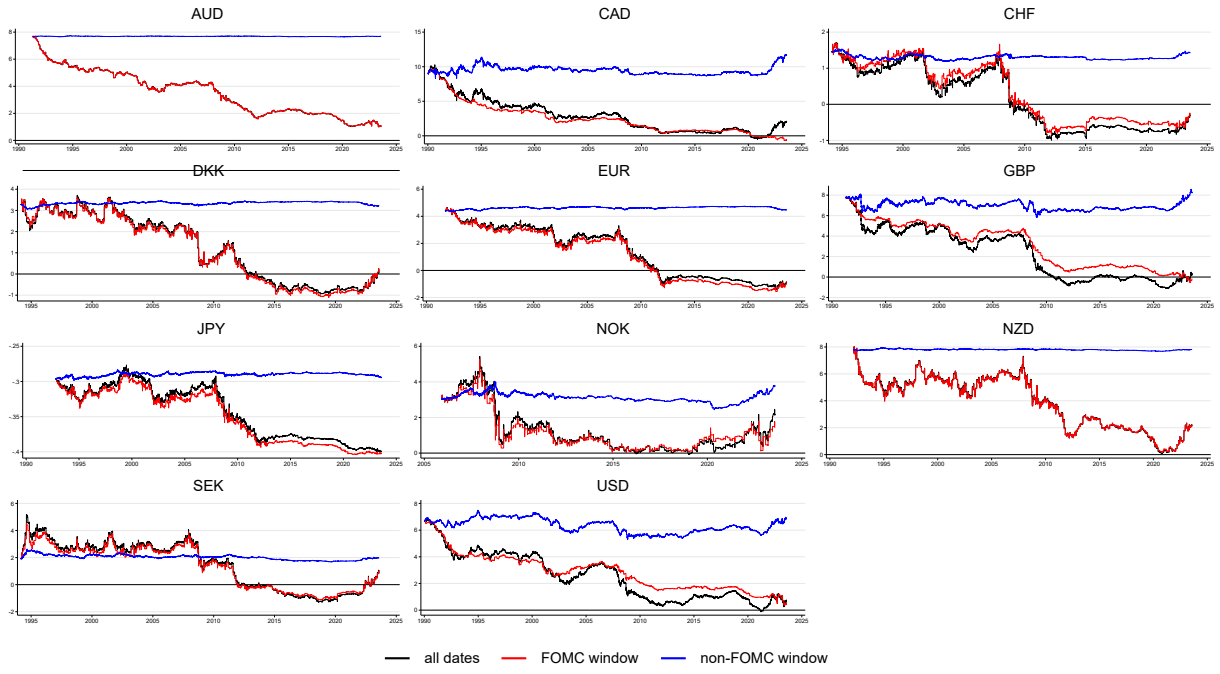

Notes: The figure plots sovereign 5-by-5-year forward risk-neutral rates and their cumulative changes during or outside FOMC windows. Each FOMC window ranges from the day before to the day after an FOMC announcement date. Non-FOMC windows are the days outside the FOMC windows.

Figure 6: FOMC announcement dates and 5-b-5-year forward term premia.

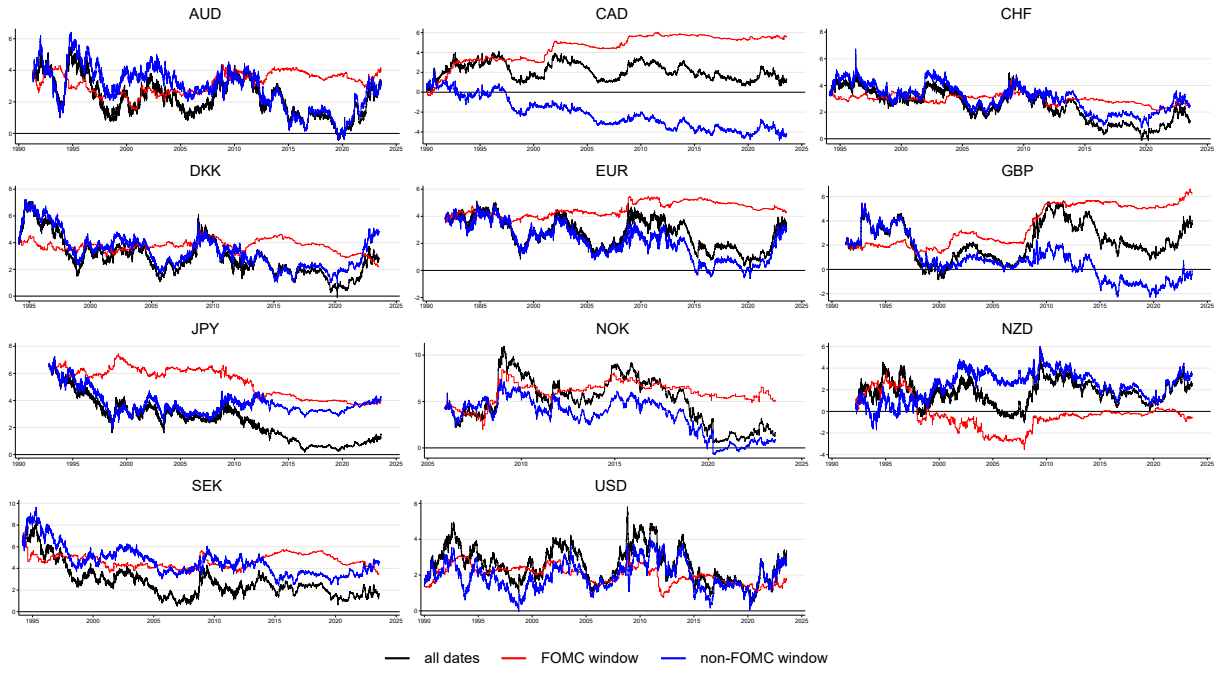

Notes: The figure plots sovereign 5-by-5-year forward term premia and their cumulative changes during or outside FOMC windows. Each FOMC window ranges from the day before to the day after an FOMC announcement date. Non-FOMC windows are the days outside the FOMC windows.

long-term interest rates into risk-neutral rates and term premia (e.g., Albagli et al. (2019), Hanson and Stein (2015)). Here, we compare the dynamics of these yield curve components estimated by OSE and FE models during FOMC announcement windows. The two models only differ in their specifications of the stochastic process of the same state vector X_t. The state process of the OSE model is described by Equation (9), where the state vector contains a random-walk component $\boldsymbol{\tau}_t$. The FE model assumes that the state process is stationary VAR(1)

$$X_t = \boldsymbol{\mu} + \Phi X_{t-1} + U_t.$$

Figure 7 shows the cumulative changes in the 5-by-5-year forward risk-neutral rates during FOMC announcement dates. The series estimated from the OSE and FE models are normalized to start at zero. Both models imply that most variations in the risk-neutral rates take place during FOMC announcement windows. However, the FE model underestimates the cumulative responses of risk-neutral rates to U.S. monetary policy announcements. For example, the FE model implies that the U.S. risk-neutral forward rate has declined by 3.4 percentage points during FOMC windows, whereas the OSE model implies a 5.7 percentage point decrease. The difference is more pronounced for other countries. The FE model implies a 1.4 percentage point decline in the U.K. risk-neutral rate during FOMC windows, while the OSE model suggests a larger decrease of 7.1 percentage points.

7 Conclusion

This paper shows that U.S. monetary policy has persistent and profound impacts on world interest rates. We provide new evidence that world interest rates are cointegrated with the cumulative effects of U.S. monetary policy announcements and that U.S. monetary policy explains the persistent variations in world interest rates. Deviations in world interest rates relative to the trend of U.S. monetary policy are consequential in predicting future interest rates and excess bond premia, and observed yields do not span this factor. We build a dynamic term structure with a stochastic trend to explain the empirical facts. The model implies that the global declines in interest rates since 1990 were mainly due to reductions in interest rate expectations, which are tied to the cumulative effects of U.S. monetary policy announcements. Ignoring the stochastic trend, as standard affine term structure models do,

Figure 7: FOMC announcement dates and 5-by-5-year forward risk-neutral rates: OSE vs. FE.

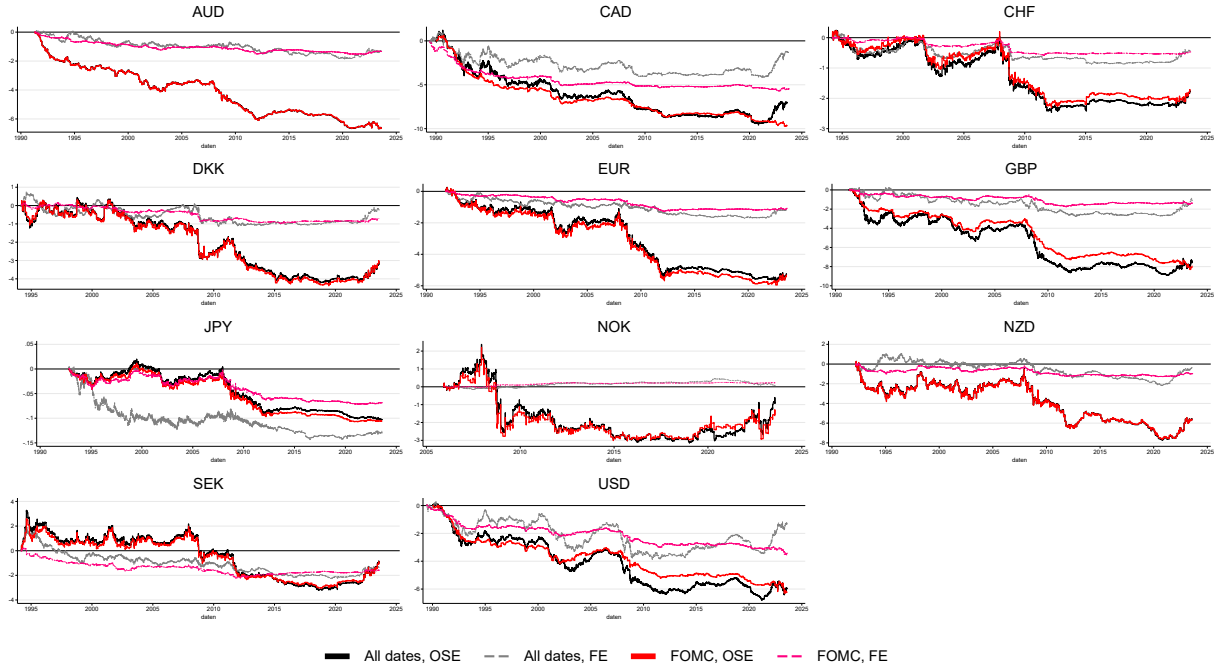

Notes: The figure plots sovereign 5-by-5-year forward risk-neutral rates and their cumulative changes during or outside FOMC windows. Each FOMC window ranges from the day before to the day after an FOMC announcement date. Non-FOMC windows are the days outside the FOMC windows. The OSE model assumes a state process $X_t = \boldsymbol{\mu} + \Gamma \boldsymbol{\tau}_t + \tilde{X}_t$, where $\boldsymbol{\tau}_t$ is a vector of random walks proxied by $(\nabla y_{loc,t}, \nabla y_{US,t})^\top$ and $\tilde{X}_t$ is a stationary VAR(1); the FE model assumes a state process $X_t = \boldsymbol{\mu} + \Phi X_{t-1} + U_t$ for the same state vector X_t.

would significantly underestimate the declines in expected interest rates and overestimate the secular declines in term premia.

References

Adrian, T., R. K. Crump, and E. Moench (2013): "Pricing the term structure with linear regressions," *Journal of Financial Economics*, 110, 110–138.

Albagli, E., L. Ceballos, S. Claro, and D. Romero (2019): "Channels of US monetary policy spillovers to international bond markets," *Journal of Financial Economics*, 134, 447–473.

Bauer, M. D. and J. D. Hamilton (2018): "Robust Bond Risk Premia," *The Review of Financial Studies*, 31, 399–448.

Bauer, M. D. and G. D. Rudebusch (2020): "Interest Rates under Falling Stars," *American Economic Review*, 110, 1316–1354.

Bauer, M. D., G. D. Rudebusch, and J. C. Wu (2014): "Term Premia and Inflation Uncertainty: Empirical Evidence from an International Panel Dataset: Comment," *American Economic Review*, 104, 323–337.

Bauer, M. D. and E. T. Swanson (2022): "A Reassessment of Monetary Policy Surprises and High-Frequency Identification," in *NBER Macroeconomics Annual 2022, volume 37*, University of Chicago Press.

Bernanke, B. (2005): "The global saving glut and the US current account deficit," Tech. rep., Board of Governors of the Federal Reserve System (US).

Bernanke, B. S., C. C. Bertaut, L. Demarco, and S. B. Kamin (2011): "International capital flows and the return to safe assets in the united states, 2003-2007," *FRB International Finance Discussion Paper*.

Caballero, R. J., E. Farhi, and P.-O. Gourinchas (2008): "An Equilibrium Model of "Global Imbalances" and Low Interest Rates," *American Economic Review*, 98, 358–393.

Carvalho, C., A. Ferrero, and F. Nechio (2016): "Demographics and real interest rates: Inspecting the mechanism," *European Economic Review*, 88, 208–226.

Cieslak, A. and P. Povala (2015): "Expected Returns in Treasury Bonds," *The Review of Financial Studies*, 28, 2859–2901.

Cochrane, J. H. and M. Piazzesi (2005): "Bond Risk Premia," *American Economic Review*, 95, 138–160.

Dedola, L., G. Rivolta, and L. Stracca (2017): "If the Fed sneezes, who catches a cold?" *Journal of International Economics*, 108, S23–S41.

Del Negro, M., G. Eggertsson, A. Ferrero, and N. Kiyotaki (2017a): "The Great Escape? A Quantitative Evaluation of the Fed's Liquidity Facilities," *American Economic Review*, 107, 824–857.

Del Negro, M., D. Giannone, M. P. Giannoni, and A. Tambalotti (2017b): "Safety, liquidity, and the natural rate of interest," *Brookings Papers on Economic Activity*, 2017, 235–316.

——— (2019): "Global trends in interest rates," *Journal of International Economics*, 118, 248–262.

Du, W., J. Im, and J. Schreger (2018): "The U.S. Treasury Premium," *Journal of International Economics*, 112, 167–181.

Eichengreen, B. (2015): "Secular stagnation: the long view," *American Economic Review*, 105, 66–70.

Gagnon, E., B. K. Johannsen, and D. Lopez-Salido (2021): "Understanding the new normal: The role of demographics," *IMF Economic Review*, 69, 357–390.

Gerko, E. and H. Rey (2017): "Monetary Policy in the Capitals of Capital," *Journal of the European Economic Association*, 15, 721–745.

Gordon, R. (2017): *The rise and fall of American growth: The US standard of living since the civil war*, Princeton University Press.

Greenwood, R. and D. Vayanos (2014): "Bond Supply and Excess Bond Returns," *The Review of Financial Studies*, 27, 663–713.

Gürkaynak, R. S., B. Sack, and E. Swanson (2005a): "Do Actions Speak Louder Than Words? The Response of Asset Prices to Monetary Policy Actions and Statements," *International Journal of Central Banking*.

——— (2005b): "The Sensitivity of Long-Term Interest Rates to Economic News: Evidence and Implications for Macroeconomic Models," *American Economic Review*, 95, 425–436.

Gürkaynak, R. S., B. Sack, and J. H. Wright (2007): "The U.S. Treasury yield curve: 1961 to the present," *Journal of Monetary Economics*, 54, 2291–2304.

Hanson, S. G. and J. C. Stein (2015): "Monetary policy and long-term real rates," *Journal of Financial Economics*, 115, 429–448.

Hillenbrand, S. (2021): "The Fed and the secular decline in interest rates," *Available at SSRN 3550593*.

Holston, K., T. Laubach, and J. C. Williams (2017): "Measuring the natural rate of interest: International trends and determinants," *Journal of International Economics*, 108, S59–S75.

Jarociński, M. (2022): "Central bank information effects and transatlantic spillovers," *Journal of International Economics*, 139, 103683.

Joslin, S., M. Priebsch, and K. J. Singleton (2014): "Risk Premiums in Dynamic Term Structure Models with Unspanned Macro Risks," *The Journal of Finance*, 69, 1197–1233, _eprint: https://onlinelibrary.wiley.com/doi/pdf/10.1111/jofi.12131.

Joslin, S., K. J. Singleton, and H. Zhu (2011): "A New Perspective on Gaussian Dynamic Term Structure Models," *The Review of Financial Studies*, 24, 926–970.

Jotikasthira, C., A. Le, and C. Lundblad (2015): "Why do term structures in different currencies co-move?" *Journal of Financial Economics*, 115, 58–83.

Krishnamurthy, A. and A. Vissing-Jorgensen (2012): "The Aggregate Demand for Treasury Debt," *Journal of Political Economy*, 120, 233–267, publisher: The University of Chicago Press.

Kuttner, K. N. (2001): "Monetary policy surprises and interest rates: Evidence from the Fed funds futures market," *Journal of Monetary Economics*, 47, 523–544.

Kuttner, N. K. (2003): "Dating changes in the federal funds rate, 1989–92," Manuscript.

Laubach, T. and J. C. Williams (2003): "Measuring the Natural Rate of Interest," *The Review of Economics and Statistics*, 85, 1063–1070, publisher: The MIT Press.

Miranda-Agrippino, S. and H. Rey (2020): "U.S. Monetary Policy and the Global Financial Cycle," *The Review of Economic Studies*, 87, 2754–2776.

——— (2022): "The Global Financial Cycle," in *Handbook of International Economics*, ed. by G. Gopinath, E. Helpman, and K. Rogoff, Elsevier, vol. 6 of *Handbook of International Economics: International Macroeconomics, Volume 6*, 1–43.

Müller, U. K. and M. W. Watson (2013): "Low-frequency robust cointegration testing," *Journal of Econometrics*, 174, 66–81.

Nakamura, E. and J. Steinsson (2018): "High-Frequency Identification of Monetary Non-Neutrality: The Information Effect*," *The Quarterly Journal of Economics*, 133, 1283–1330.

Rey, H. (2015): "Dilemma not Trilemma: The Global Financial Cycle and Monetary Policy Independence," Working Paper 21162, National Bureau of Economic Research.

Stock, J. H. and M. W. Watson (1993): "A Simple Estimator of Cointegrating Vectors in Higher Order Integrated Systems," *Econometrica*, 61, 783–820, publisher: [Wiley, Econometric Society].

Summers, L. H. (2014): "Reflections on the 'new secular stagnation hypothesis'," *Secular stagnation: Facts, causes and cures*, 1, 27–40.

Svensson, L. E. (1994): "Estimating and Interpreting Forward Interest Rates: Sweden 1992 - 1994," .

Wright, J. H. (2011): "Term Premia and Inflation Uncertainty: Empirical Evidence from an International Panel Dataset," *American Economic Review*, 101, 1514–1534.

A Monetary Policy Announcement Dates

Table A1 and Table A2 list the dates of scheduled and unscheduled FOMC meetings, respectively, that serve as date t for the FOMC window.

June 1989 - December 1993. The federal funds rate became the sole target of U.S. monetary policy in late 1989. The Fed relied on open market operations to signal any monetary policy changes. Kuttner (2001, 2003) thoroughly examined the market's reaction to monetary policy news between June 1989 and June 2008. His analysis allows us to determine the dates when the market learned about the outcomes of scheduled and unscheduled FOMC meetings associated with changes in the federal funds rate target. For scheduled meetings that did not result in changes to the federal funds rate, we use the day after the meeting as the relevant date.

1994 - . Since 1994, there has been a high degree of transparency in monetary policy decisions. From 1994 to 1997, the Federal Reserve issued statements for scheduled FOMC meetings if there were changes in the federal funds rate target. Since 1998, statements have been released for every scheduled meeting. These statements clearly communicate the federal funds rate target and are typically released on the day of the meeting. To capture the market's knowledge of monetary policy decisions, we use the actual date of the FOMC meeting as it aligns with the date that the market learns about these decisions. Additionally, the majority of monetary policy decisions have been made during scheduled meetings since 1994. We exclude unscheduled meetings unrelated to monetary policy[6], which were often focused on money market functioning, and also exclude unscheduled meetings for which the Fed did not issue a statement. Thus, my final sample includes all unscheduled meetings related to monetary policy for which the Fed released a statement, ensuring a comprehensive analysis.

[6]This is common in the literature, such as Kuttner (2001). The dates excluded are August 10, 2007, August 16, 2007, January 21, 2008, March 10, 2008, May 9, 2009, October 4, 2019, March 19, 2020, March 23, 2020, and March 31, 2020.

Table A1: Scheduled FOMC Meeting Dates

		Scheduled FOMC Meetings							
Year	N	1.	2.	3.	4.	5.	6.	7.	8.
1989	5				7-Jul	23-Aug	4-Oct	15-Nov	20-Dec
1990	8	8-Feb	28-Mar	16-May	5-Jul	22-Aug	3-Oct	14-Nov	18-Dec
1991	8	7-Feb	27-Mar	15-May	5-Jul	21-Aug	2-Oct	6-Nov	18-Dec
1992	8	6-Feb	1-Apr	20-May	2-Jul	19-Aug	7-Oct	18-Nov	23-Dec
1993	8	4-Feb	24-Mar	19-May	8-Jul	18-Aug	22-Sep	17-Nov	22-Dec
1994	8	4-Feb	22-Mar	17-May	6-Jul	16-Aug	27-Sep	15-Nov	20-Dec
1995	8	1-Feb	28-Mar	23-May	6-Jul	22-Aug	26-Sep	15-Nov	19-Dec
1996	8	31-Jan	26-Mar	21-May	3-Jul	20-Aug	24-Sep	13-Nov	17-Dec
1997	8	5-Feb	25-Mar	20-May	2-Jul	19-Aug	30-Sep	12-Nov	16-Dec
1998	8	4-Feb	31-Mar	19-May	1-Jul	18-Aug	29-Sep	17-Nov	22-Dec
1999	8	3-Feb	30-Mar	18-May	30-Jun	24-Aug	5-Oct	16-Nov	21-Dec
2000	8	2-Feb	21-Mar	16-May	28-Jun	22-Aug	3-Oct	15-Nov	19-Dec
2001	8	31-Jan	20-Mar	15-May	27-Jun	21-Aug	2-Oct	6-Nov	11-Dec
2002	8	30-Jan	19-Mar	7-May	26-Jun	13-Aug	24-Sep	6-Nov	10-Dec
2003	8	29-Jan	18-Mar	6-May	25-Jun	12-Aug	16-Sep	28-Oct	9-Dec
2004	8	28-Jan	16-Mar	4-May	30-Jun	10-Aug	21-Sep	10-Nov	14-Dec
2005	8	2-Feb	22-Mar	3-May	30-Jun	9-Aug	20-Sep	1-Nov	13-Dec
2006	8	31-Jan	28-Mar	10-May	29-Jun	8-Aug	20-Sep	25-Oct	12-Dec
2007	8	31-Jan	21-Mar	9-May	28-Jun	7-Aug	18-Sep	31-Oct	11-Dec
2008	8	30-Jan	18-Mar	30-Apr	25-Jun	5-Aug	16-Sep	29-Oct	16-Dec
2009	8	28-Jan	18-Mar	29-Apr	24-Jun	12-Aug	23-Sep	4-Nov	16-Dec
2010	8	27-Jan	16-Mar	28-Apr	23-Jun	10-Aug	21-Sep	3-Nov	14-Dec
2011	8	26-Jan	15-Mar	27-Apr	22-Jun	9-Aug	21-Sep	2-Nov	13-Dec
2012	8	25-Jan	13-Mar	25-Apr	20-Jun	1-Aug	13-Sep	24-Oct	12-Dec
2013	8	30-Jan	20-Mar	1-May	19-Jun	31-Jul	18-Sep	30-Oct	18-Dec
2014	8	29-Jan	19-Mar	30-Apr	18-Jun	30-Jul	17-Sep	29-Oct	17-Dec
2015	8	28-Jan	18-Mar	29-Apr	17-Jun	29-Jul	17-Sep	28-Oct	16-Dec
2016	8	27-Jan	16-Mar	27-Apr	15-Jun	27-Jul	21-Sep	2-Nov	14-Dec
2017	8	1-Feb	15-Mar	3-May	14-Jun	26-Jul	20-Sep	1-Nov	13-Dec
2018	8	31-Jan	21-Mar	2-May	13-Jun	1-Aug	26-Sep	8-Nov	19-Dec
2019	8	30-Jan	20-Mar	1-May	19-Jun	31-Jul	18-Sep	30-Oct	11-Dec
2020	7	29-Jan	29-Apr	10-Jun	29-Jul	16-Sep	5-Nov	16-Dec	
2021	8	27-Jan	17-Mar	28-Apr	16-Jun	28-Jul	22-Sep	3-Nov	15-Dec
2022	8	26-Jan	16-Mar	4-May	15-Jun	27-Jul	21-Sep	2-Nov	14-Dec

Table A2: Unscheduled FOMC Meeting Dates

		Unscheduled FOMC Meetings								
Year	N	1.	2.	3.	4.	5.	6.	7.	8.	9
1989	4				5-Jun	26-Jul	16-Oct	6-Nov		
1990	3	13-Jul	29-Oct	7-Dec						
1991	9	8-Jan	1-Feb	8-Mar	30-Apr	6-Aug	13-Sep	31-Oct	6-Dec	20-Dec
1992	2	9-Apr	4-Sep							
1993	0									
1994	1	18-Apr								
1995	0									
1996	0									
1997	0									
1998	1	15-Oct								
1999	0									
2000	0									
2001	3	3-Jan	18-Apr	17-Sep						
2002	0									
2003	0									
2004	0									
2005	0									
2006	0									
2007	0									
2008	2	22-Jan	8-Oct							
2009	0									
2010	0									
2011	0									
2012	0									
2013	0									
2014	0									
2015	0									
2016	0									
2017	0									
2018	0									
2019	0									
2020	2	3-Mar	15-Mar							
2021	0									

B The Shifting Endpoint Model

B.1 Details of the No-Arbitrage Recursions

First, we show that the state vector Z_t evolves as

$$Z_t = \boldsymbol{\mu}_Z + \Phi_Z Z_{t-1} + V_t, \quad V_t \equiv \begin{bmatrix} \boldsymbol{\eta}_t \\ U_t \end{bmatrix}, \tag{A1}$$

with

$$\boldsymbol{\mu}_Z = \begin{bmatrix} 0 \\ (I-\Phi)\boldsymbol{\mu} \end{bmatrix}, \quad \Phi_Z = \begin{bmatrix} I_{K_\tau} & 0_{K_\tau \times K_X} \\ (I-\Phi)\Gamma & \Phi \end{bmatrix}, \quad \Omega_V \equiv \mathbf{E}[V_t V_t^\top] = \begin{bmatrix} \Omega_\eta & \Omega_\eta \Gamma^\top \\ \Gamma\Omega_\eta & \Omega \end{bmatrix}.$$

We rewrite Z_t as

$$Z_t = \begin{bmatrix} 0 \\ \boldsymbol{\mu} \end{bmatrix} + \begin{bmatrix} I_{K_\tau} & 0_{K_\tau \times K_X} \\ \Gamma & \Phi \end{bmatrix} \begin{bmatrix} \boldsymbol{\tau}_{t-1} \\ \tilde{X}_{t-1} \end{bmatrix} + \begin{bmatrix} \boldsymbol{\eta}_t \\ \Gamma \boldsymbol{\eta}_t + \tilde{U}_t. \end{bmatrix}$$

Note that

$$\begin{bmatrix} \boldsymbol{\tau}_{t-1} \\ \tilde{X}_{t-1} \end{bmatrix} = \begin{bmatrix} 1 & 0_{K_\tau \times K_X} \\ -\Gamma & I \end{bmatrix} \begin{bmatrix} \boldsymbol{\tau}_{t-1} \\ X_{t-1} \end{bmatrix} - \begin{bmatrix} 0 \\ \boldsymbol{\mu} \end{bmatrix}.$$

Substituting for $\boldsymbol{\tau}_{t-1}$ and $\tilde{X}_{t-1}$, we get $\boldsymbol{\mu}_Z, \phi_Z$ and V_t. Since $V_t \perp \tilde{U}_t$, the expression for Ω_V follows naturally.

Next, we show that restriction (12) implies the bond pricing equation (13). We prove by guess-and-verify. The no-arbitrage recursion is

$$p_t^{(n)} = \mathbf{E}_t[m_{t+1}] + \mathbf{E}_t[p_{t+1}^{(n-1)}] + \frac{1}{2}\mathbf{Var}_t(m_{t+1}) + \frac{1}{2}\mathbf{Var}_t(p_{t+1}^{(n-1)}) + \mathbf{Cov}_t(m_{t+1}, p_{t+1}^{(n-1)}). \tag{A2}$$

Note that $\mathbf{E}_t[\cdot]$ refers $\mathbf{E}[\cdot|Z_t]$, and

$$\begin{aligned} \mathbf{E}_t[X_{t+1}] =& \boldsymbol{\mu} + \Gamma\boldsymbol{\tau}_t + \Phi\tilde{X}_t = \boldsymbol{\mu} + \Gamma\boldsymbol{\tau}_t + \Phi(X_t - \boldsymbol{\mu} - \Gamma\boldsymbol{\tau}_t) \\ =& (I-\Phi)(\boldsymbol{\mu} + \Gamma\boldsymbol{\tau}_t) + \Phi X_t. \end{aligned}$$

When $p_t^{(n)} = \mathcal{A}_n + \mathcal{B}_n^\top X_t$,

$$\mathbf{E}_t[m_{t+1}] + \frac{1}{2}\mathbf{Var}_t(m_{t+1}) = -\delta_0 - \boldsymbol{\delta}_1^\top X_t,$$

$$\mathbf{E}_t[p_{t+1}^{(n-1)}] = \mathcal{A}_{n-1} + \mathcal{B}_{n-1}^\top[(I-\Phi)(\boldsymbol{\mu} + \Gamma\boldsymbol{\tau}_t) + \Phi X_t],$$

$$\mathbf{Var}_t(p_{t+1}^{(n-1)}) = \mathcal{B}_{n-1}^\top \Omega \mathcal{B}_{n-1},$$

$$\mathbf{Cov}_t(m_{t+1}, p_{t+1}^{(n-1)}) = -\mathcal{B}_{n-1}^\top(\Lambda_0 + \Lambda_1 Z_t).$$

Note that $\Lambda_1 Z_t = \Lambda_{11}\boldsymbol{\tau}_t + \Lambda_{12} X_t$, and we hope to eliminate $\boldsymbol{\tau}_t$ from the right-hand side of the recursion. Collecting the terms involving $\boldsymbol{\tau}_t$, we should have

$$\mathcal{B}_{n-1}^\top[(I-\Phi)\Gamma - \Lambda_{11}] = 0, \quad \forall n.$$

So $\Lambda_{11} = (I-\Phi)\Gamma$ eliminates $\boldsymbol{\tau}_t$ from the right-hand side of Equation (A2).

Finally, we derive the bond pricing recursions. Equation (A2) together with Equation (12) implies

$$\begin{aligned} p_t^{(n)} =& -\delta_0 - \boldsymbol{\delta}_1^\top X_t + \mathcal{A}_{n-1} + \mathcal{B}_{n-1}^\top[(I-\Phi)\boldsymbol{\mu} + \Phi X_t] && \text{(A3)} \\ &+ \frac{1}{2}\mathcal{B}_{n-1}^\top \Omega \mathcal{B}_{n-1} - \mathcal{B}_{n-1}^\top(\Lambda_0 + \Lambda_{12} X_t). && \text{(A4)} \end{aligned}$$

So,

$$\begin{aligned} \mathcal{A}_n =& \mathcal{A}_{n-1} - \delta_0 + \mathcal{B}_{n-1}^\top(I-\Phi)\boldsymbol{\mu} + \frac{1}{2}\mathcal{B}_{n-1}^\top \Omega \mathcal{B}_{n-1} - \mathcal{B}_{n-1}^\top \Lambda_0, && \text{(A5)} \\ \mathcal{B}_n^\top =& -\boldsymbol{\delta}_1^\top + \mathcal{B}_{n-1}^\top(\Phi - \Lambda_{12}). && \text{(A6)} \end{aligned}$$

The yields are

$$y_t^{(n)} = A_n + B_n^\top X_t, \tag{A7}$$

with $A_n = -\frac{1}{n}\mathcal{A}_n$ and $B_n = -\frac{1}{n}\mathcal{B}_n$.

Table A3: RMSE of the monthly OSE model.

	AUD	CAD	CHF	DKK	EUR	GBP	JPY	NOK	NZD	SEK	USD
1	1.46	1.51	1.59	1.25	1.46	0.51	1.03	0.52	0.72	1.08	0.55
2	1.20	0.70	1.50	1.16	1.52	0.37	2.05	0.47	1.47	1.21	0.43
3	0.65	0.87	0.86	0.94	1.20	0.49	1.00	0.29	0.75	1.02	0.42
4	1.43	0.81	1.31	1.45	1.92	0.55	1.75	0.34	1.32	1.72	0.46
5	1.46	0.64	1.17	1.25	1.63	0.37	2.14	0.45	1.09	1.58	0.25
6	1.57	0.72	1.15	1.68	1.56	0.46	3.06	0.65	0.97	1.39	0.34
7	2.91	0.86	2.23	2.89	3.36	0.58	4.75	1.21	1.65	1.85	0.50
8	4.70	0.81	3.26	4.15	5.30	0.48	6.93	3.16	2.08	2.39	0.44
9	6.37	0.93	3.73	5.42	6.72	0.48	9.79	6.48	2.03	3.18	0.39
10	8.45	1.86	5.73	7.52	8.98	1.30	14.06	9.19	4.57	5.80	0.99
Mean	3.50	1.22	2.45	3.14	3.87	0.59	5.40	3.15	1.78	2.41	0.56

Notes: Root mean squared errors of yield curve fitting, in basis points. For each country, we report the RMSE for the 1-, 2-, ..., 10-year maturities and the mean RMSE across all maturities.

B.2 Model Fit

In the main text, we estimated three sets of models: the baseline monthly OSE and ESE models, and the daily OSE model for investigating the dynamics of risk-neutral rates during FOMC windows. In Table A3, Table A4, and Table A5, we report the root mean squared errors of yield curve fitting. Specifically, we compute the squared difference between the yield data and model-implied yields. We then compute the square root of the average squared difference over the full sample. For each country, we report the RMSE associated with the 1-, 2-, ..., 10-year maturities and the mean RMSE across all maturities.

Table A4: RMSE of the monthly ESE model.

	AUD	CAD	CHF	DKK	EUR	GBP	JPY	NOK	NZD	SEK	USD
1	2.93	1.49	3.00	3.01	1.78	0.55	3.86	0.67	0.86	1.13	0.58
2	1.22	0.80	3.28	1.28	1.92	0.36	2.84	0.44	1.61	1.31	0.42
3	0.78	1.00	2.19	0.90	1.62	0.50	2.21	0.21	0.81	1.20	0.50
4	2.13	1.20	2.61	2.82	1.81	0.56	2.38	0.14	1.38	1.63	0.60
5	2.68	0.76	2.61	3.80	1.50	0.35	1.77	0.24	1.16	1.31	0.42
6	2.68	0.64	2.14	4.19	0.97	0.41	0.95	0.25	0.91	0.80	0.39
7	2.83	0.85	2.07	4.76	1.84	0.53	1.21	0.32	1.32	1.22	0.47
8	3.41	0.65	2.21	6.25	2.77	0.42	1.54	0.56	1.52	1.43	0.37
9	4.77	0.56	3.48	9.79	3.32	0.27	1.66	1.16	0.85	0.91	0.29
10	8.65	1.88	6.97	17.20	6.43	1.10	4.61	1.96	3.78	3.30	0.99
Mean	3.83	1.06	3.36	7.11	2.82	0.55	2.56	0.80	1.65	1.57	0.54

Notes: Root mean squared errors of yield curve fitting, in basis points. For each country, we report the RMSE for the 1-, 2-, ..., 10-year maturities and the mean RMSE across all maturities.

Table A5: RMSE of the daily OSE model.

	AUD	CAD	CHF	DKK	EUR	GBP	JPY	NOK	NZD	SEK	USD
1	2.97	4.48	2.75	2.22	1.90	1.29	3.19	1.05	0.79	1.19	0.85
2	1.26	3.35	2.86	1.49	2.31	1.01	2.63	0.68	1.52	1.35	0.66
3	0.73	3.44	1.82	0.93	2.33	1.12	2.42	0.83	0.80	1.11	0.99
4	2.06	3.20	2.33	2.35	2.38	1.23	2.33	1.10	1.36	1.91	1.04
5	2.51	2.75	1.99	2.56	1.82	1.05	1.75	0.87	1.05	1.61	0.97
6	2.47	2.40	1.71	2.31	1.06	0.86	1.23	0.39	0.69	0.94	1.05
7	2.78	2.19	1.86	2.33	1.69	0.74	1.46	0.61	1.28	1.29	1.20
8	3.63	2.03	2.19	2.74	2.50	0.51	1.79	0.41	1.64	1.52	1.27
9	5.33	2.19	3.44	4.25	3.10	0.29	1.95	1.64	1.23	0.84	1.31
10	9.41	3.17	6.23	8.51	6.10	1.22	4.62	2.87	3.78	3.66	1.59
Mean	3.55	3.45	2.81	3.15	2.63	1.03	2.34	1.16	1.59	1.91	1.16

Notes: Root mean squared errors of yield curve fitting, in basis points. For each country, we report the RMSE for the 1-, 2-, ..., 10-year maturities and the mean RMSE across all maturities.